FINITE ELEMENT MODEL OF COMPOSITE CONNECTIONS STRENGTHENED WITH CFRP LAMINATES

MAHYAR RAMEZANI

MASTER PROJECT REPORT SUBMITTED IN PARTIAL FULFILMENT
OF THE REQUIREMENTS FOR THE DEGREE OF
MASTER OF ENGINEERING

FACULTY OF ENGINEERING AND BUILT ENVIRONMENT
UNIVERSITI KEBANGSAAN MALAYSIA
BANGI

2013

MODEL UNSUR TERHINGGA SAMBUNGAN KOMPOSIT DIPERKUATKAN DENGAN LAPISAN CFRP

MAHYAR RAMEZANI

LAPORAN PROJEK SARJANA YANG DIKEMUKAKAN UNTUK MEMENUHI SEBAGAHIAN DARIPADA SYARAT MEMPEROLEH IJAZAH SARJANA KEJURUTERAAN

FAKULTI KEJURUTERAAN DAN ALAM BINA
UNIVERSITI KEBANGSAAN MALAYSIA
BANGI

2013

DECLARATION

I hereby declare that the work in this thesis is my own except for quotations and summaries which have been duly acknowledged.

20 August 2013

MAHYAR RAMEZANI
P60836

ACKNOWLEDGEMENTS

I wish to express my sincere appreciation to my parents for their support during my postgraduate years at UKM. I would also like to thank my brother, my sister and my friends who have supported me. My gratitude extends beyond words.

ABSTRACT

Carbon Fiber Reinforced Polymer (CFRP) materials are being widely used for structural applications. Despite the relatively high cost of the CFRP materials, their high strength-to-weight ratio and corrosion resistance as well as easy handling and installation have made them widely popular for different civil engineering applications where increased strength and/or ductility is important. This thesis investigates the moment-rotational response of an endplate composite connection including strengthening of the slab by using different sizes and thickness of CFRP sheets in hogging moment regions and different reinforcement bar ratios by using finite element simulations. A three dimensional non-linear model is developed in ANSYS to study the feasibility of decreasing the reinforcing bars in the presence of the CFRP laminate in hogging moment regions of the slab. The verification of the analysis is carried out to calibrate the un-strengthened model by available experimental results obtained from a series of composite connection tests as reported by other researchers. The moment resistance for the partial depth endplate composite connection obtained by ANSYS 12.1 software is found to be very close to the corresponding laboratory test value. From the results it can be observed that applying CFRP sheets to the tension face of composite slab can reduce the amount of steel reinforcement bars required for flexural strength of composite connections.

ABSTRAK

Carbon Fiber Reinforced Polymer (CFRP) adalah bahan yang kini digunakan secara meluas untuk aplikasi struktur. Walaupun kos CFRP agak mahal, nisbah kekuatan-kepada-berat adalah tinggi dan rintangan kakisan serta pengendalian dan pemasangan yang mudah telah menjadikannya amat popular dalam aplikasi kejuruteraan awam yang berbeza di mana kekuatan meningkat dan / atau kemuluran adalah penting. Tesis ini mengkaji tindak balas momen-putaran sambungan plat hujung komposit termasuk pengukuhan papak dengan menggunakan pelbagai saiz dan ketebalan kepingan CFRP dalam kawasan momen negatif dan nisbah bar tetulang yang berbeza. Model unsur terhingga tiga dimensi tak lelurus dibangunkan menggunakan perisian ANSYS untuk mengkaji kesan CFRP dengan mengurangkan nisbah tetulang terhadap isipadu konkrit. Model unsure terhingga telah ditentusahkan dengan keputusan eksperimen. Daripada keputusan ia boleh diperhatikan bahawa kepingan CFRP boleh mengurangkan penggunan jumlah bar tetulang keluli yang diperlukan.

TABLE OF CONTENTS

LIST OF TABLES

LIST OF FIGURES

List of symbols

M	Moment capacity
M_s	Contribution of moment capacity from reinforcement bars
M_b	Contribution of moment capacity from bolts
Φ	Rotation capacity
$S_{j.ini}$	Initial stiffness of the joint
q	Uniformly distributed load
L_b	Span of the beam
p_y	Yield strength
f_c'	Concrete compressive strength
f_{cu}	Compressive cube strength of concrete
f_r	Concrete tensile strength
f_1	Width of beam flange
F_t	Bolt tensile strength
d_c	Depth of concrete slab
$[K]$	Overall stiffness matrix
$[Ke]$	Element stiffness matrix
$[D]$	Material property matrix
$[B]$	Shape function matrix
E	Elastic modulus
G	Shear modulus
ν	Poisson's ratio

CHAPTER I

INTRODUCTION

1.1 BACKGROUND OF COMPOSITE CONSTRUCTION

Concrete and structural steel are the two most widely used materials in the construction industry. Each of these materials has their own strength and weaknesses. Concrete is usually desired for its high strength in compression, high buckling resistance and fire resistance; however its tensile resistance is insufficient. Structural steel sections are also very strong in tension and ductile; however they are susceptible to buckling. The negative properties of these materials can be discarded when they are combined to form a composite structure. In this way, the benefits of these two materials can be optimally used. Composite structures refer to any members composed of more than one material. The components of these composite members are rigidly connected such that no relative movement can occur. For example, efficient and economical light weight floor systems could be created by integrating the structural properties of concrete and cold-formed steel decking by ensuring composite action through shear connectors welded to the structural steel and embedded in concrete, as shown in Figure 1.1.

The term composite structure normally implies to the use of steel and concrete formed together into a component in such a way that the resulting arrangement, functions as a single item (Nethercot *et al.* 2003). Composite beams are the most common form of composite members used in composite construction. The design of composite beams incorporating composite slabs is affected by the shape and orientation of the decking, as indicated in Figure 1.2. The ability of a metal deck to contribute tensile resistance is included only when the decking is oriented parallel to the direction of the beam (Xiao *et al*. 1994).

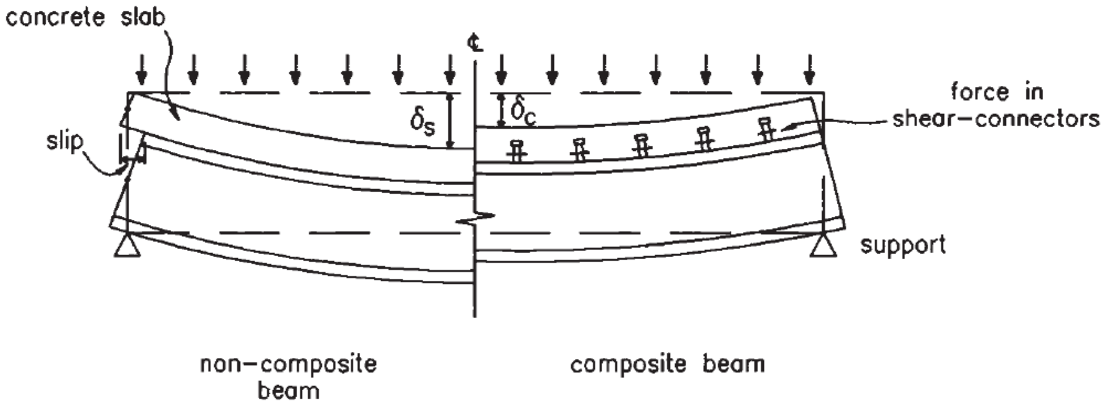

Figure 1.1 Composite and non-composite action (Xiao and Nethercot 1994)

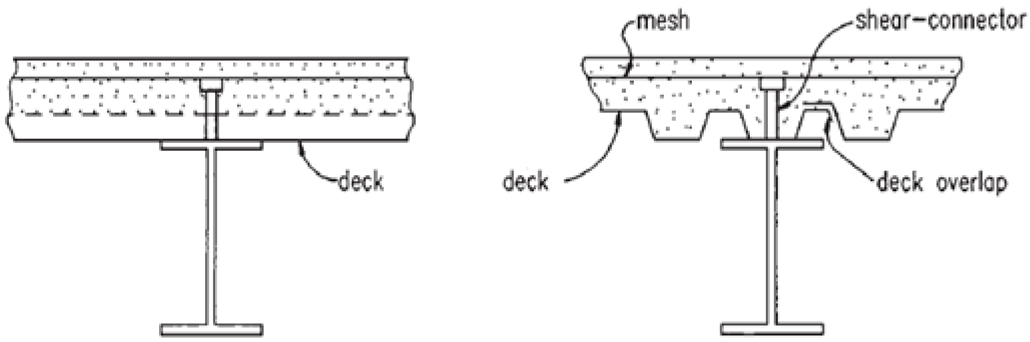

(a) (b)

Figure 1.2 Composite beams incorporating composite deck slabs (a) deck perpendicular to beam, (b) deck parallel to beam (Xiao and Nethercot 1994)

Nethercot *et al.* (2003) stated that the definition of a composite beams can be taken as elements resisting only flexure and shear that comprise of two longitudinal components connected together either continuously or by a series of discrete connectors. In this case, the concrete slab is connected to the steel section and both act compositely in carrying the load. The slip between the slab and the steel section is prevented and the connection resists a longitudinal shear force. The strain is assumed to vary linearly over the full depth of a composite cross section as can be seen in Figure 1.3.

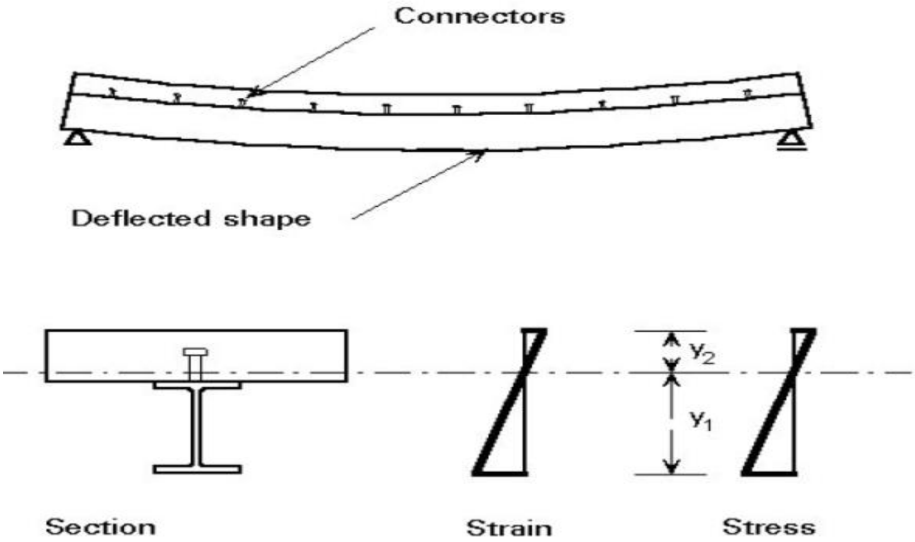

Figure 1.3 Composite action

Composite beams may be formed by either completely encasing a steel member in concrete with the composite action depending upon the natural bond between steel and concrete, or by connecting the concrete floor to the top flange of the steel framing member by shear connectors (Viest *et al*. 1997). Figure 1.4 shows a composite beam and the stress distribution for hogging and sagging bending. It is known that in the hogging region the concrete slab is not effective due to cracking. To produce the necessary tensile force, a significant contribution from the reinforcement is required.

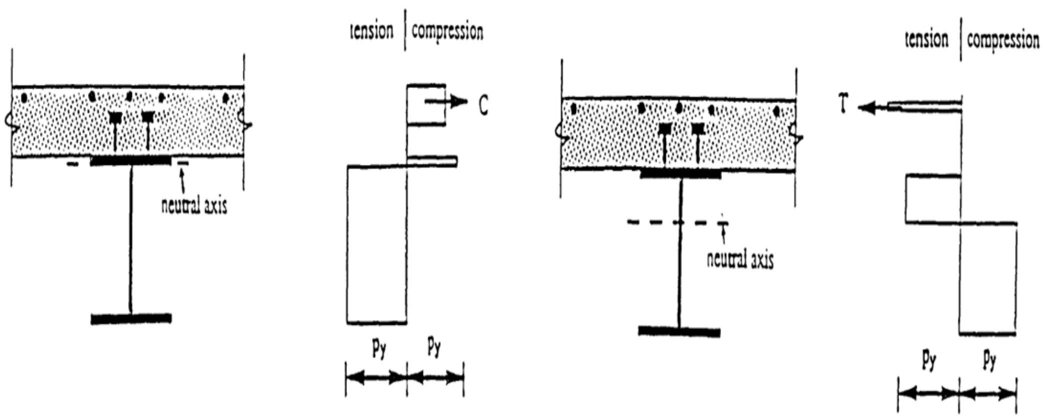

(a) sagging bending (b) hogging bending

Figure 1.4 Composite beam in (a) sagging and (b) hogging bending

1.2 COMPOSITE CONNECTION

Composite connections may be regarded as the addition of the reinforced concrete slab with a proper shear transfer mechanism between the steel beam and the concrete slab. Before the introduction of composite beams in the 1970's, frames were designed as bare steel frames. With the introduction of composite beams, the design of composite frames started. Figure 1.5 shows a few types of connections that are used to form the joint between the beam and the column. Figure 1.6 shows the typical composite details. The connection types that are used in composite construction are:

a) End-plate
b) Fin-plate
c) Angle cleated

Endplate connections can be:

- Partial depth endplate
- Flush endplate
- Extended endplate

Angle cleated connections can be:

- Web side cleat (single or double)
- Top or bottom cleat
- Combination of web and top or bottom cleat

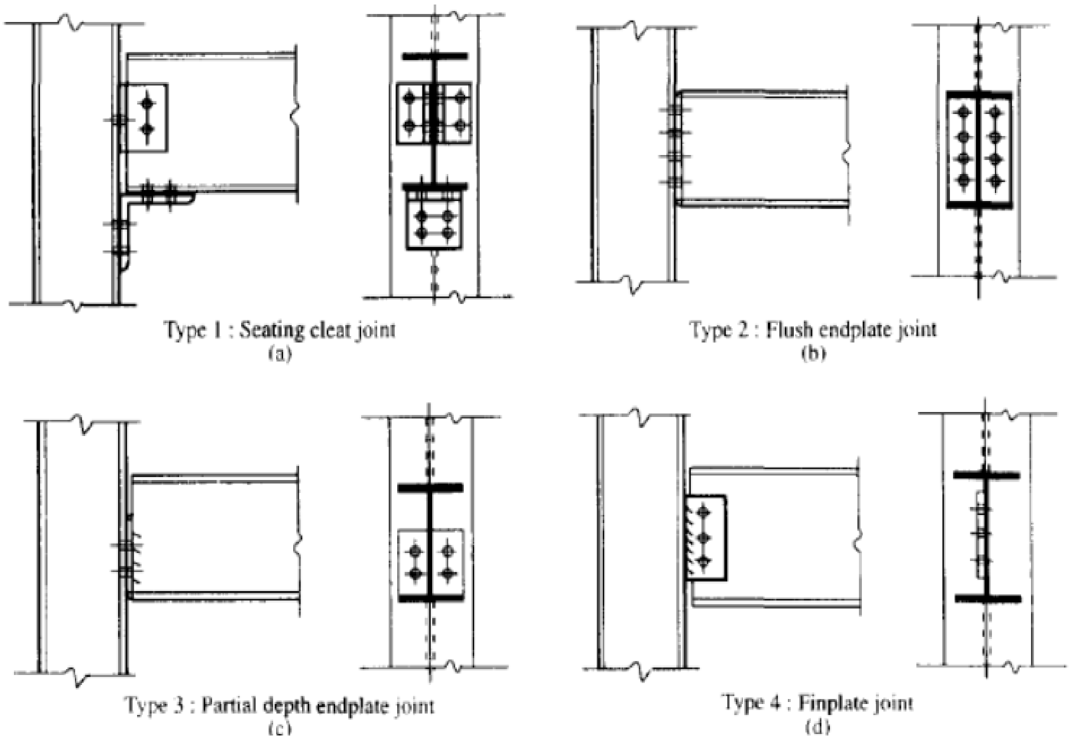

Figure 1.5 Types of beam to column connections (Xiao and Nethercot 1994)

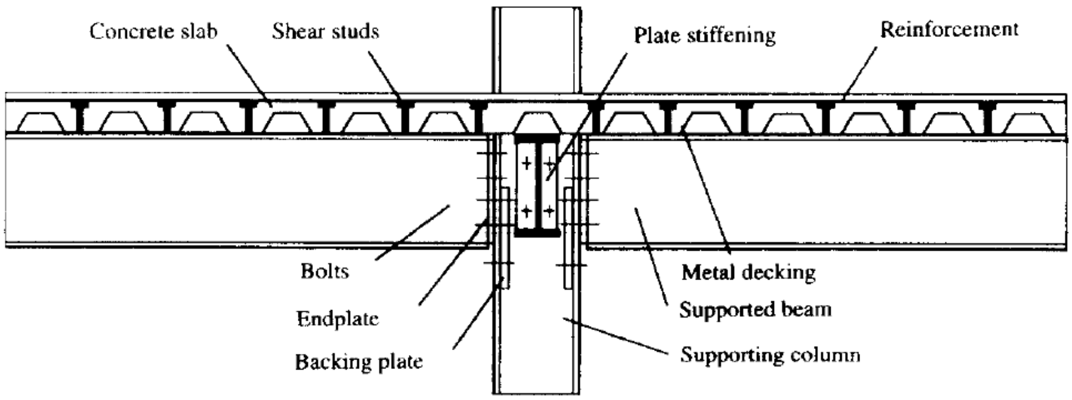

Figure 1.6 Cruciform arrangement of composite connection (Xiao and Nethercot 1994)

According to the most consolidated definition (Bijlaard *et al*. 1989; Nethercot and Zandonini 1990; Kirby *et al*. 1990), the connection is the physical component which mechanically fastens the beam to the column and is concentrated at the location where the fastening action occurs. The joint, however, is the connection plus the corresponding zone of interaction between the connected members (the panel zone of the column web) as shown in Figures 1.7 and 1.8.

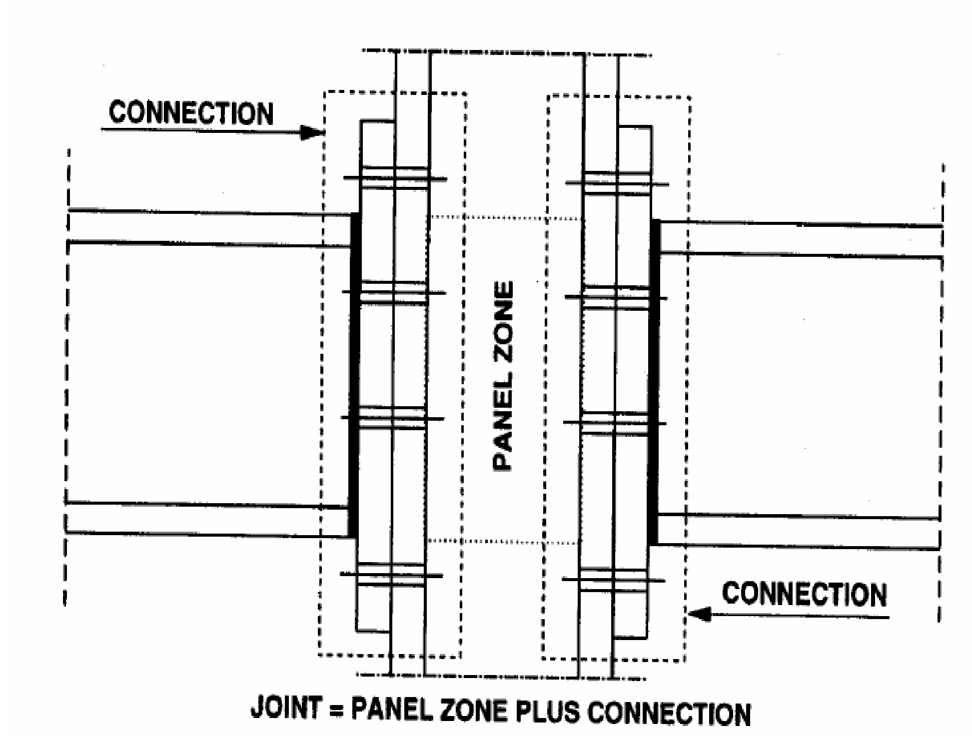

Figure 1.7 Distinction between joint and connection (Nethercot and Zandonini 1990)

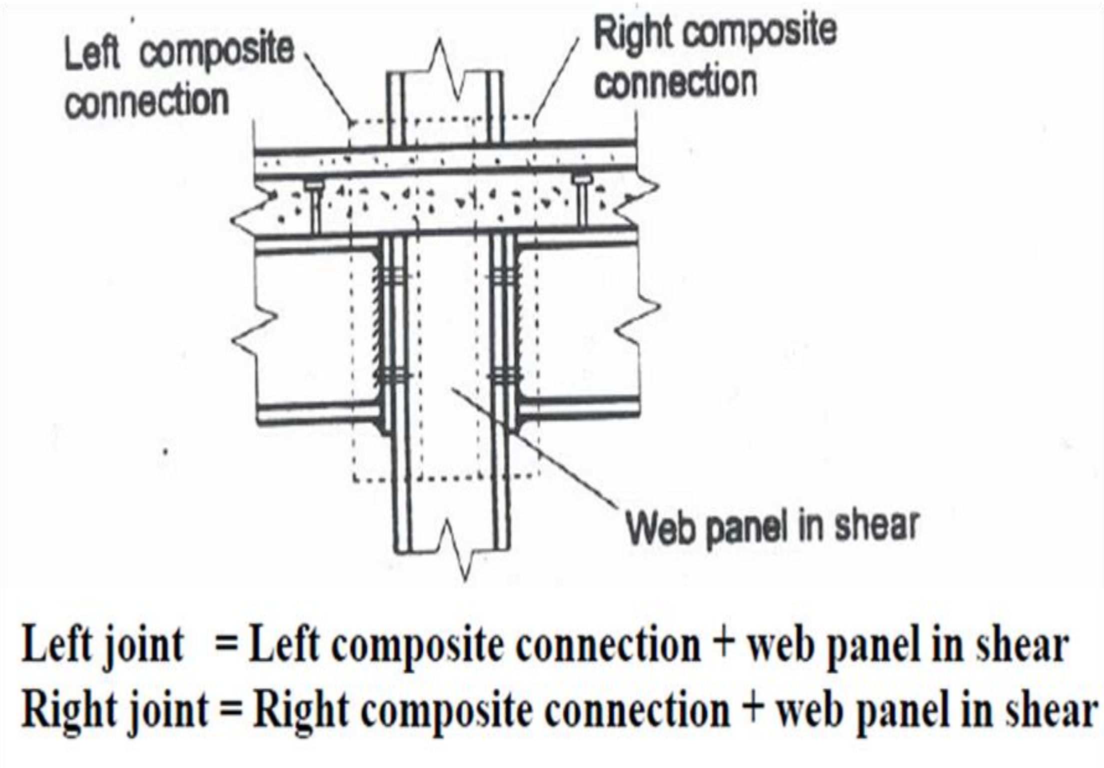

Figure 1.8 Parts of a beam-to-column joint configuration
Source: Proposed Annex J, Eurocode4

Joint characteristics described by moment (M) - rotation (Φ) curve. Three key parameters of a joint are:

- Moment capacity
- Rotation capacity
- Rotational stiffness

Knowledge of these fundamental properties is necessary before the true semi-rigid and partial strength nature of the connections can be properly incorporated into more realistic methods of composite connections and frame design. The conventional design approach used by most engineers is based on one of two extreme assumptions: The fixed connection model and the hinged connection model. However, in real applications, the actual stiffness of a connection always falls between these two extremes (i.e. the connection will behave in a semi-rigid manner). Also the capacity of an un-stiffened connection might be less than that of the connected beam in which case it is called *"*partial strength.*"*

Figure 1.9 shows the moment diagram for a beam loaded with a uniformly distributed load q, having span of L_b with different support conditions. It is clear from the Figure 1.9 that the assumption of a pinned connection overestimates the span moment and deflections and underestimates the support moment. A rigid connection assumption underestimates the mid span moment and deflection, while it overestimates the support moment. Also, it can be seen that the sum of the connection moment and the span moment is always equal to $\frac{qL_b{}^2}{8}$.

Therefore, by evaluating the connection moment capacity, it would be possible to design the members more efficiently. After the formation of a plastic hinge at the connection, the moment may be redistributed to the mid span, in such a way that the sum of the connection moment capacity and the mid span moment is still $\frac{qL_b{}^2}{8}$.

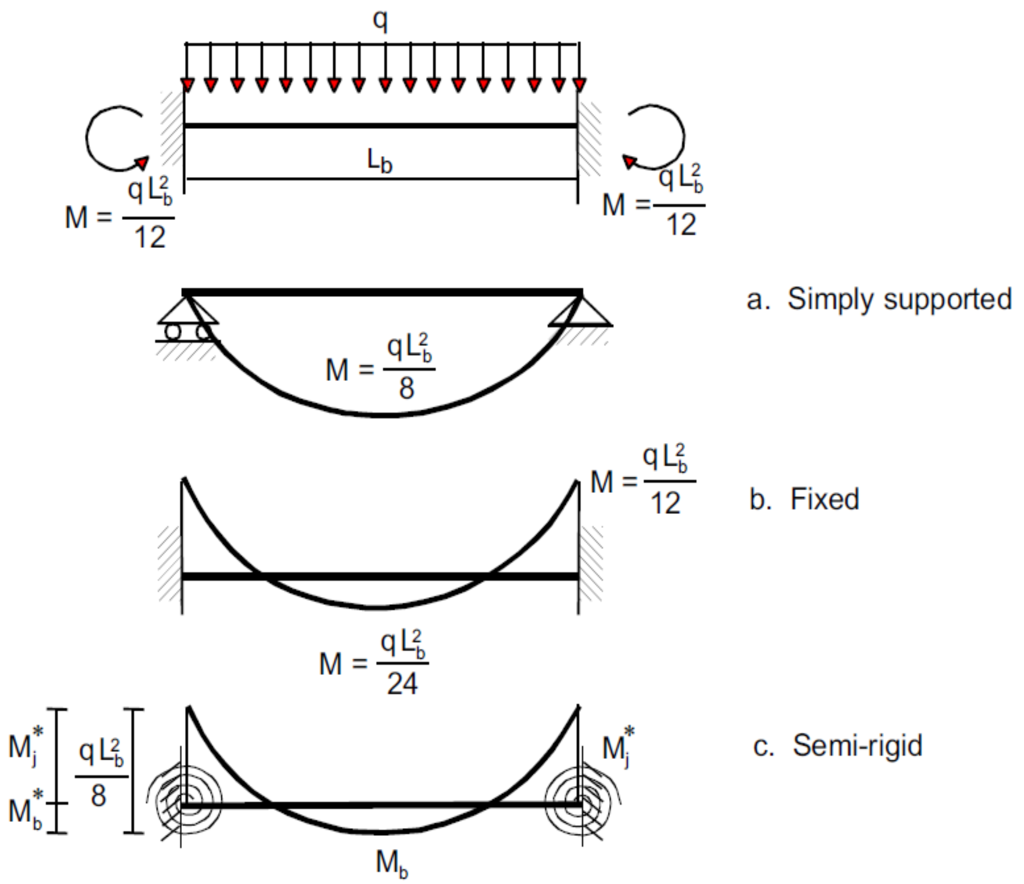

Figure 1.9 Moment diagram of a beam with uniformly distributed load and different support conditions

1.3 RETROFITTING WITH FRP LAMINATES

The Fiber Reinforced Polymer (FRP) composites consist of high strength fibers embedded in a matrix of polymer resin as shown in Figure 1.10. The fibers are generally carbon, glass, or aramid in a matrix such as vinylester or epoxy. These materials are performed to form plates under factory conditions, generally by the pultrusion process.

The typical values for properties of the fibers are given in Table 1.1. These fibers are all linear elastic up to failure. The primary functions of the matrix in a composite are to transfer stresses between the fibers to provide a barrier against the environment and to protect the surface of the fibers from the mechanical abrasion.

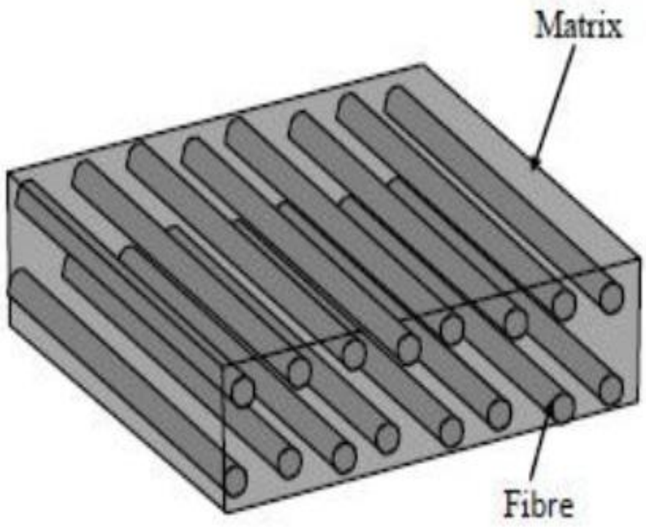

Figure 1.10 Schematic representation of a unidirectional FRP plate

Table 1.1 Typical properties of the fibers (Feldman 1989, Kim 1995)

Material	Elastic modulus (GPa)	Tensile strength (MPa)	Ultimate tensile strain (%)
Carbon			
High strength	215-235	3500-4800	1.4-2.0
Ultra high strength	215-235	3500-6000	1.5-2.3
High modulus	350-700	2100-2400	0.5-0.9
Ultra high modulus	500-700	2100-2400	0.2-0.4
Glass			
E	70	1900-3000	3.0-4.5
S	85-90	3500-4800	4.5-5.5
Aramid			
Low modulus	70-80	3500-4100	4.3-5.0
High modulus	115-130	3500-4000	2.5-3.5

The mechanical properties of composites depend on the fiber properties, matrix properties, fiber-matrix bond properties, fiber content and fiber orientation. A composite with all fibers in one direction is designated as unidirectional. If the fibers are oriented in many directions, the composite is bidirectional or multidirectional. The approximate stiffness and strength of a unidirectional Carbon Fiber Reinforced Polymer (CFRP) with a 65 % volume fraction of carbon fiber is given in Table 1.2. As a comparison the corresponding properties for steel are also given.

Table 1.2 Typical properties of prefabricated FRP strips and comparison with steel

Material	Elastic modulus (GPa)	Tensile strength (MPa)	Ultimate tensile strain (%)
	E_f	f_f	ε_{fu}
Prefabricated strips			
Low modulus CFRP strips	170	2800	1.6
High modulus CFRP strips	300	1300	0.5
Mild steel	200	400	25 (yield strain = 0.2%)

Adhesives are used to attach the composites to other surfaces such as concrete. The most common adhesives are acrylics, epoxies and urethanes. The epoxies provide high bond strength with high temperature resistance, whereas acrylics provide moderate temperature resistance with good strength and rapid curing.

Most of the FRP systems used nowadays consist of carbon fibers embedded in an epoxy matrix. Actually, there are many reasons that make carbon fibers one of the most attractive alternatives for post strengthening concrete structures. Considering all reinforcing fiber materials used to produce FRPs, the carbon fibers have the highest specific modulus and strength that provides a great stiffness to the system. Therefore, they are an ideal choice to be applied in structures sensitive to weight and deflection. Compared with steel, carbon fibers can be about five times lighter and present a tensile strength of eight to ten times higher.

1.4 PROBLEM STATEMENT

Reinforced concrete structures often have to face modification and improvement of their performance during their service life. The FRP materials are not adversely affected by weather and salts. Therefore, the composite laminate will not be subjected to problems associated with corrosion as in the case of steel reinforcing bars. In addition, the laminate can act as a protective cover at the joint by reducing the exposed concrete surface area where moisture or salts can penetrate into the joint and cause corrosion of reinforcing bars. Therefore, FRP products can be used in the initial construction or for structural repair/strengthening of existing structures. The strengthening is required when there are increased applied loads, human errors in initial construction, or when a structural member loses its strength due to deterioration over time.

In the last decade, the development of strong epoxy glue has led to a technique which has great potential in the field of upgrading structures. Basically, the technique involves attaching steel plates or FRP plates to the surface of the concrete. The plates then act compositely with the concrete and help to carry the loads.

FRP can be convenient compared to steel for a couple of reasons. These materials have higher ultimate strength and lower density than steel. The installation is easier and temporary support until the adhesive gains its strength is not required due to their low weight. In addition, they can be formed into complicated shapes and can be easily cut to length on the job site.

Therefore, this thesis aims to study the behavior of composite connections retrofitted with CFRP sheets in hogging moment regions of the slab. In the past, experimental approach has been widely used to investigate the behavior of composite connections. But full scale testing of composite connections are expensive, time consuming and sometimes difficult to perform. An alternative is to use finite element analysis but the results need to be calibrated against good experimental test data. A three dimensional non-linear finite element analysis has therefore been developed as an alternative method to study the behavior of end-plate composite connections. The moment (M) – rotation (Φ) curve is plotted and compared with the experimental results done by Xiao (1994) at the university of Nottingham.

1.5 OBJECTIVES OF THE STUDY

The objectives of this study are as follows:

1. To develop a nonlinear finite element analysis in order to study the moment-rotational response of endplate composite connections using ANSYS software.

2. To predict the moment-rotational response of endplate composite connections including strengthening of the slab by using different sizes and thickness of CFRP sheets in hogging moment regions of the slab.

3. To investigate on feasibility of decreasing the reinforcing bars in the presence of the CFRP laminates in hogging moment regions of the slab.

1.6 SCOPE OF THE STUDY

The real behavior of the composite connection can be obtained by using the experimental results. Nevertheless, according to the special features of this project such as cost and time limitations and lack of laboratory equipment, the finite element method is used.

1.7 OUTLINE OF THE THESIS

Chapter 2 provides a chronological review of earlier research on composite connections. The review includes a summary of both the experimental and analytical investigations.

In chapter 3, the methodology used in the ANSYS 12.1 software to model and analyze all composite connections are explained in detail. The modeling, attributes, geometry, meshing, boundary conditions, loading and material properties are among the important factors mentioned in this section. Moreover, a brief explanation of nonlinear solution procedures using ANSYS software is discussed in this chapter.

The results obtained from the analysis and discussions are included in chapter 4. Finally, chapter 5 presents the conclusions and recommendations for future studies.

CHAPTER II

LITERATURE REVIEW

2.1 INTRODUCTION

The semi-rigid joint action on the behavior of steel frames has received considerable attention since the 1980s (Nethercot 1986) and the same concept also applies to composite frames. The recognition of the semi-rigid concept is a great advancement in joint studies because of its realistic representation of joint behavior and economic gain in frame design compared with conventional assumptions of perfectly rigid or pinned joints. In the case of beam-to-column joints, the behavior can be modeled by moment-rotation curves (M-Φ curves).

A composite connection is a combination of the bare steel connection and a reinforced concrete slab acting together and sharing the loads. It is therefore essential to understand the behavior of the bare steel connection in order to properly understand the behavior of the composite connections. A large number of tests have been performed on bare steel connections since the 1930's. Nethercot and Zandonini (1989) made a review of the prediction methods for the bare steel connections. Generally, the extended endplate connection gives the highest moment capacity and stiffness, while the web cleat connections provide the lowest. The M-Φ curve illustrates the relationship between the moment transmitted by the joint and the rotation of the joint due to that moment. Typical M-Φ curves are shown for these connections in Figure 2.1 using the same beam and column combination.

The perfectly pinned and rigid assumptions adopted in conventional design are corresponding to *x* and *y* axes of a M-Φ curve, respectively. Accurate and economical structural analysis can only be performed if the knowledge of the actual M-Φ characteristics including moment capacity, rotational stiffness and rotation capacity of the joint is available. However, such characteristics of the joint are rather complex and a more comprehensive understanding of joint response especially joint stiffness and rotation capacity is required.

The reason for the high moment capacity of the extended endplate connection is that the lever arm is largest for this connection. The moment-rotation curves shown in Figure 2.1 are idealized. In reality, they may not be so smooth due to the slip of the bolts and local buckling of components. The structural members are generally composed of relatively thin elements. The slender nature of these thin elements results in susceptibility to local buckling under compressive stress. The classifications from BS 5950 of plastic, compact, semi-compact, and slender are replaced in Eurocode3 with class 1, class 2, class 3 and class 4 respectively. Figure 2.2 shows the effect of local buckling on the moment-rotational behavior of the connection.

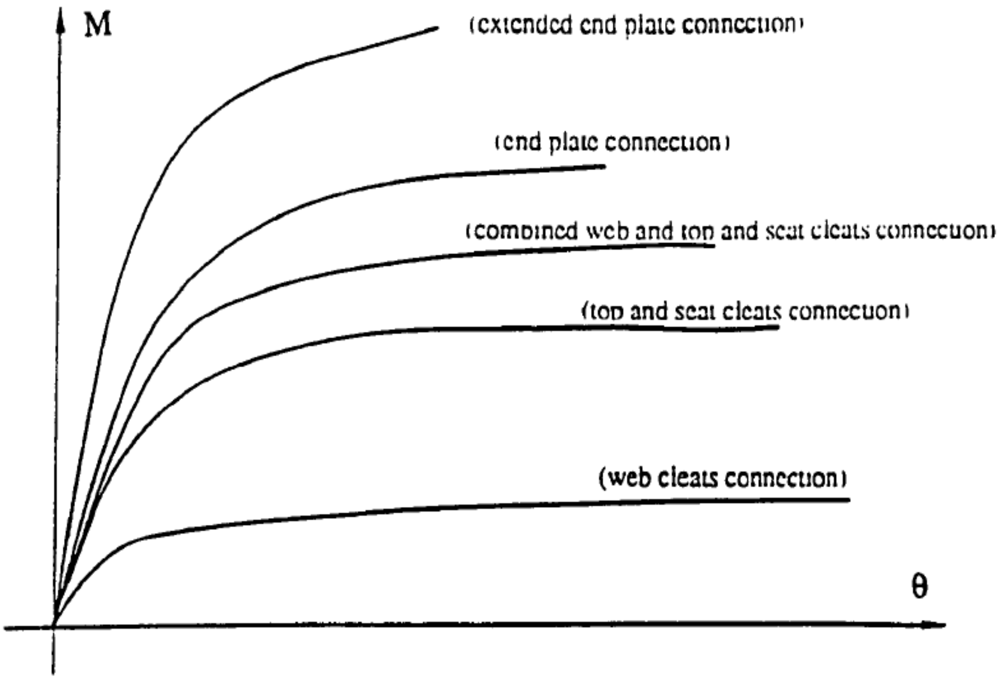

Figure 2.1 Typical M-Φ curves of commonly used steelwork connection

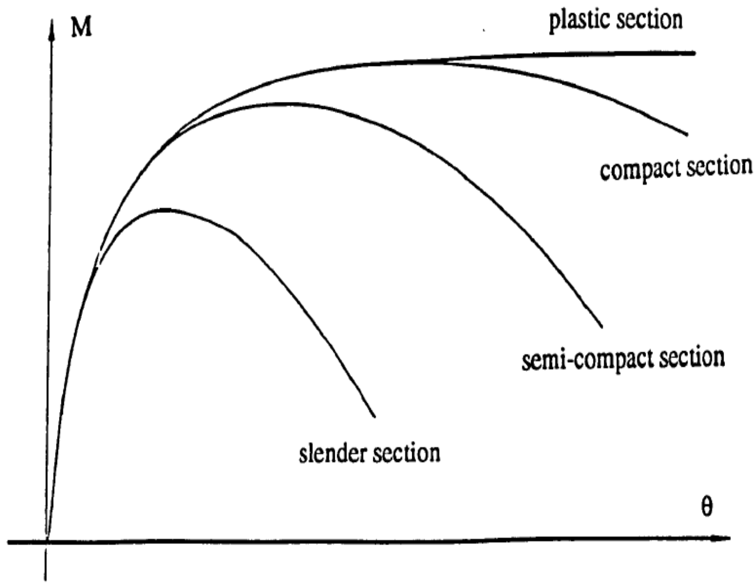

Figure 2.2 Effect of steel beam section class on the connection's M-Φ curves

2.2 CLASSIFICATION OF COMPOSITE CONNECTIONS

Three approaches for the design of a structure in which the behavior of the connection is fundamental are given in Eurocode3 and BS 5950. The three methods are: simple design, continuous design and semi-continuous design. Eurocode3, Part 1.1, states that the appropriate type of joint model depends on the classification of the joint and the method of global analysis. This is shown in Table 2.1.

Table 2.1 Type of joint model (Eurocode3 Part 1.1, Annex J)

Method of Global Analysis	Classification of joints		
Elastic	Nominally pinned	Rigid	Semi-rigid
Rigid - Plastic	Nominally pinned	Full-Strength	Partial-strength
Elastic - Plastic	Nominally pinned	Rigid and Full-Strength	Semi-rigid and partial-strength Semi-rigid and full-strength Rigid and partial-strength
Type of Joint Model	Simple	Continuous	Semi-continuous

Classifying of the connections according to its stiffness is called elastic analysis. In Eurocode3 Part 1.1, Annex J, it is recommended that connections can be classified by stiffness, comparing the initial stiffness of the joint $(S_{j.ini})$ with the limits given in Figure 2.3.

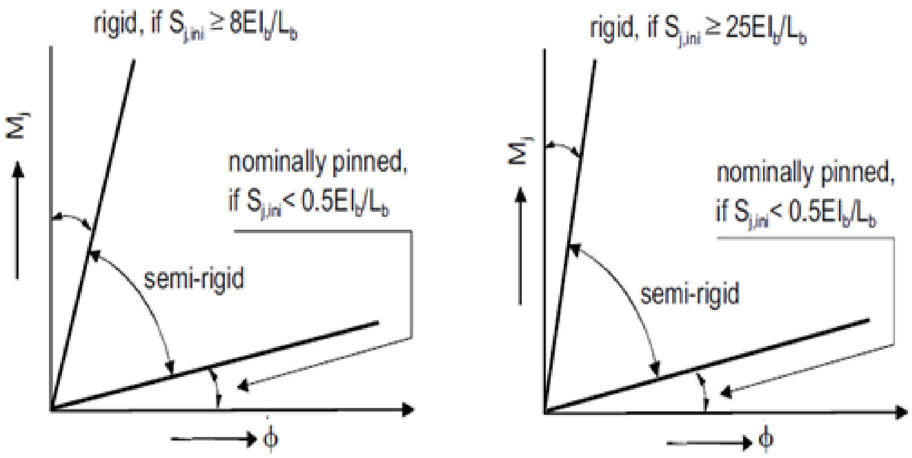

(a) Braced frames (b) Unbraced frames

Figure 2.3 Boundaries for stiffness classification of composite connections (Eurocode3 Part 1.1, Annex J)

Plastic analysis is used when the connections are classified according to strength. For classification by strength the connection is compared with the capacity of the connected beam to identify which of the two members will fail first (i.e., the connection or the beam) (Nethercot *et al*. 2003). While elastic-plastic analysis is used when the connections are classified according to both their stiffness and strength. For a simple design, no matter which method of global analysis is applied, the joints are classified as nominally pinned. The implication of this is that the connection is sufficiently flexible to restrict the development of end fixity (i.e., no end moments exist). For continuous design, the connections can be classified as rigid, full-strength or rigid and full-strength depending on whether elastic analysis, rigid-plastic analysis or elastic-plastic analysis is employed. According to Nethercot *et al*. (2003), the term full-strength relates the strength of the connection to that of the connected beam. If the moment capacity of the connection is higher than that of the connected beam, the connection is termed full-strength. The purpose of this comparison is to determine whether the joint or the connected member will limit the resistance of the structure.

Rigid and full-strength joints which are a result of using elastic-plastic analysis are supposed to withstand moment, shear force and axial load without a change in the angle between members. By using continuous design, usually beam sizes decreases but the need to supply joints with rigidity arises to cancel out the possible economic benefits.

While simple design ignores stiffness and continuous design only allows full-strength connections, the semi-continuous design accepts the fact that most practical connections are capable of providing some degree of stiffness and their moment capacity may be limited (Nethercot *et al*. 2003). According to BS 5950 (2000), this method (semi-continuous design) may be used where joints have some degree of strength and stiffness, but insufficient to develop full continuity. Similar to continuous design, the joints are classified differently according to the type of a global analysis. Here, the term partial-strength refers to connections that have a lower moment capacity compared with the connected beam. This will result in the connection failure before the connected beam fails.

The classification of connections according to strength and stiffness are illustrated in Figures 2.4 and 2.5, respectively. From the moment rotation ($M-\Phi$) curves, connections 1 and 2 can be classified as full strength because their moment capacities exceed that of the connecting beam. Conversely, moment capacities for connections 3 and 5 are lower than the connecting beam, thus are termed as partial strength. According to stiffness, connections 1, 2, 3 and 4 are classified as rigid, connection 5 as semi-rigid and connection 6 as nominally pinned.

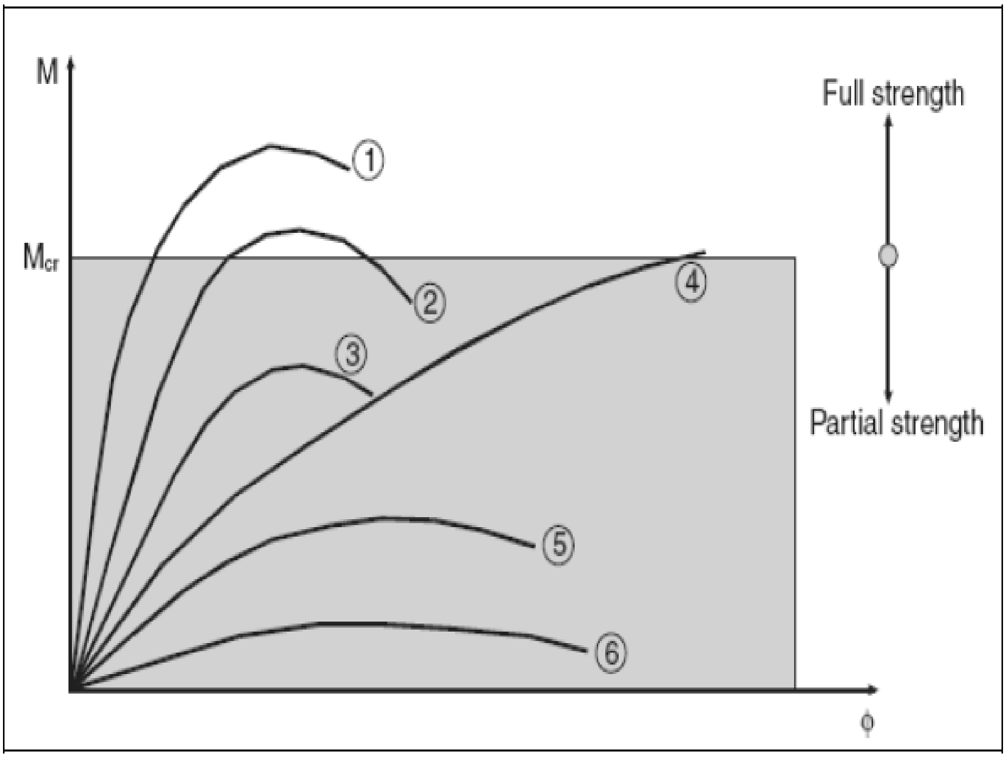

Figure 2.4 Classification of composite connections by strength

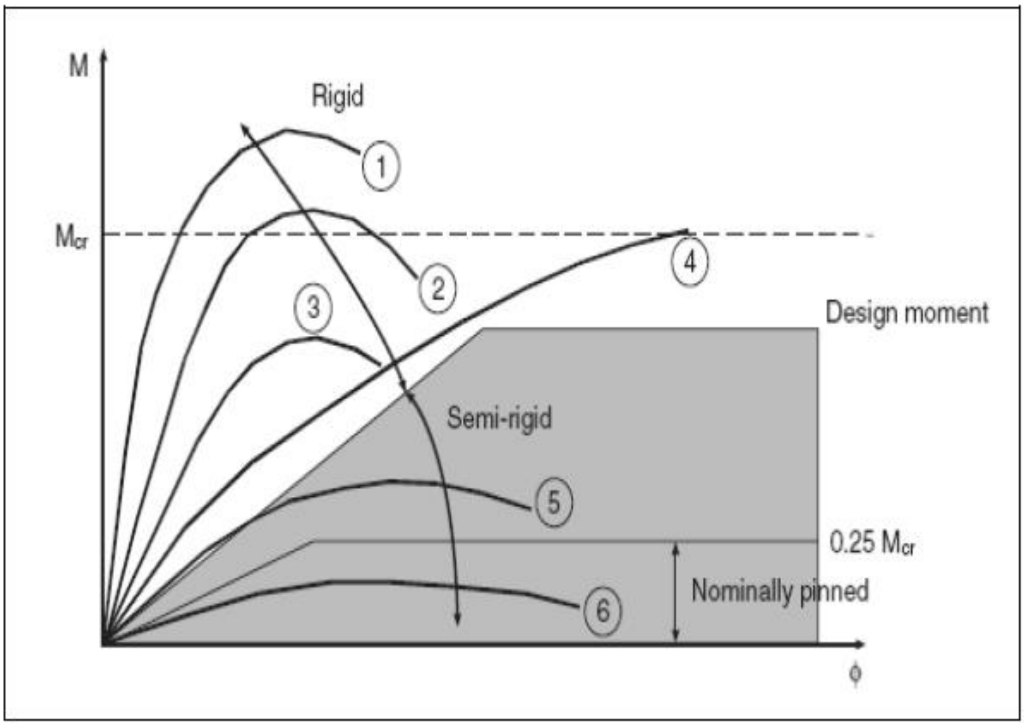

Figure 2.5 Classification of composite connections by stiffness

2.3 STUDY ON COMPOSITE CONNECTIONS

The study of semi-rigid composite connections started in 1970. Since then numerous composite connection tests have been done around the world. Using the test results, attempts were made to produce simplified prediction methods. Equations for moment capacity and rotation capacity have been proposed on the basis of the test results. The numerical studies have also been performed. This section describes briefly the experimental and analytical work carried out in this field to study the moment capacity and rotation capacity of composite connections.

The interaction between the composite slab and the components of the steel connection makes the connection behavior more complicated than the bare steel connections. To clearly understand such response the direct method is to carryout full scale tests. The results of experimental work not only provide understanding of the response of the composite connections, but also supply the necessary information for comparison against the analytical and numerical works. The first tests on semi-rigid composite connections were conducted by Johnson and Hope-Gill in 1972. They conducted five tests on composite cleated connections with flat slabs. The most important works on the subject up to 1989 were revised by Zandonini and summarized by Simoes da Silva *et al*. Simoes da Silva (1989) also revised the experimental results carried out between 1990 and 2001. Loh *et al*. (2004) compiled the experimental results carried out up to 2004.

Composite connections may be regarded as simply the addition of the reinforced concrete slab with a proper shear transfer mechanism between the steel beam and the concrete slab. All the test results have shown that the addition of reinforcement near the column, increases the moment capacity and the stiffness of the connections. This is also due to the increase in the lever arm of the internal forces in the connection. But the percentage increase may be different for different types of connections for the same percentage increase of reinforcement. Xiao's (Xiao *et al*., 1994) test SCJ8, SCJ9 and SCJ10 used partial depth endplates at the top, middle and at the bottom of the beam, respectively. It was observed that SCJ8 gave the lowest moment capacity, whereas SCJ10 gave the highest moment capacity. This is due to the fact that the position of the endplate controls the length of the lever arm. The moment capacity of a composite connection as was observed in the tests was affected by the reinforcement ratio, symmetry and non-symmetry of the applied load, degree of shear interaction provided (using shear studs), shear to moment ratio, column characteristics and column axis connection.

A considerable number of experiments and analytical works on composite connections have been carried out at the University of Nottingham since 1994. Xiao *et al*. (1994) have performed numerous large-scale experiments and Ahmed and Nethercot (1997) have carried out analytical studies by using the Finite Element Method. From the experimental testing, Xiao *et al*. (1994) concluded that the key properties of composite connections were dramatically affected by many parameters such as slab depth, joint type, reinforcement ratio, etc. The desirable connection behavior can be achieved by adjusting these parameters.

- **REINFORCEMENT RATIO**

Usually, up to a certain limit, the higher the reinforcement ratio the higher the moment capacity of the connection is. Tests by Benussi *et al*. (1989) , Xiao (1994) , Anderson and Najafi (1991) have confirmed this. Xiao's (1994) test SCJ3 and SCJ4 had the same steel detailing but the reinforcement ratios were 0.2% and 1% and the moment capacity was increased by 136%. The inclusion of large quantities of reinforcement into the slab may increase the moment resistance. But to achieve this, tensile force generated by the moment must be balanced by the compression force acting on the lower part of the beam-to-column connection. Otherwise, a strong tensile capacity with weak compression resistance will not be able to generate the required moment capacity, making it unnecessary to increase the slab reinforcement.

- **LOAD APPLICATION PROCEDURE**

The studies and analyses of the joints is undertaken with the eventual aim of using such joints in frames. In a real structure, the joint is usually loaded non-symmetrically.

Most of the tests on the composite connections have been symmetrical. But, tests by Puhali *et at*. (1990) indicated that non-symmetric application of the load affects the behavior of the composite joints. Tests by Benussi *et al*. (1989) and Law (1983) showed that unbalanced moments on the two sides of the column also affects the connection behavior. Tests by Li *et al*. (1994) showed that the effect of non-symmetrical moment on the connection moment capacity is significant only when the non-symmetrical moment ratio is quite high compared with the column web shear resistance or the concrete strength.

- **SHEAR CONNECTORS**

Most of the tests on composite connections have been carried out using a uniform distribution of shear connectors and full shear connection between the reinforced slab and the steel beam top flange. This makes it difficult to interpret the exact role played by the shear connectors in the composite connections. Tests conducted by Law (1983) employed uniformly distributed shear connectors on one side of the connection and a non uniform distribution of shear connectors on the other side of the connection. The test results indicated that a different interaction between the steel beam and the concrete slab slightly affected the connection behavior in the early stage, but significantly in the non-linear part. Najafi and Anderson (1991) conducted tests with partial shear interaction and full shear interaction. The results indicated that the partial strength connections had low moment capacity and initial stiffness with respect to the full interaction. It was observed from these tests that changing to a composite connection dramatically increased the initial stiffness and the moment capacity.

- **COLUMN CHARACTERISTICS**

If the column web is weak compared with other components of the connection, it may lead to the buckling of its web if no stub beam is attached to the column web. Also the thickness of the column web determines the compressive force that can be sustained by a column web. Xiao's (Xiao *et al.*, 1994) test SCJ4 reached its ultimate capacity due to the buckling of the column web. But, test SCJ6 which had a web stiffener, developed an increased moment capacity by 19%.

- **EFFECT OF COLUMN AXIS CONNECTION**

Xiao *et al*. (1994) conducted a total of four tests (SCJ13, SCJ14, SCJ18 and SCJ19) with column minor axis connection. The equivalent connections for SCJ13 and SCJ14 for major axis connections are SCJ10 and SCJ8. The obtained moment capacities were 147.8 kN.m and 181.4 kN.m for SCJ10 and SCJ13, respectively. The reason for the increased moment capacity of SCJ13 is that SCJ10 reached its ultimate moment due to the buckling of the column web, which was prevented in the case of SCJ13. The moment capacity was 89.8 kN.m for SCJ14 and it was 84 kN.m for SCJ8. Note that both connections reached their ultimate moment capacity due to the buckling of the beam web. It appears that as long as the compressive forces can be resisted and the column web buckling can be prevented by means of stub beams, there is no effect of this factor on the moment capacity of composite cruciform connections. Tests SCJ18 and SCJ19 were cantilever joints where both connections failed due to the insufficient anchorage of the reinforcement causing failure of the concrete slab.

2.4 PREDICTION OF MOMENT AND ROTATION CAPACITY OF COMPOSITE CONNECTIONS USING EQUATIONS

Xiao *et al*. (1994) tested 19 composite connections and used the findings to develop a mathematical model to predict both the moment capacity and the rotation capacity of composite cleated connections, composite fin-plate connections, and composite flush endplate connections. Reduction factors according to EC4 clause 4.4.3 and BS5950 Part 1 Clause 4.2.6 were recommended for use when high beam shear was present. Separate equations were proposed to calculate the moment capacity of the connection when its compressive capacity was governed by the column.

Knowledge of the potential tensile and compressive resistances available from the slab and the beam permits the location of the neutral axis to proceed. Four cases are available:

- Neutral axis within the concrete slab
- Neutral axis within the beam's upper flange

- Neutral axis within the beam's web above the top row of bolts
- Neutral axis within the beam's web below the top row of bolts

Amongst which, the last case is more likely to occur. In this case, some of the bolt rows will be in tension and will therefore augment the tensile resistance. The position of neutral axis for this case is shown in Figure 2.6.

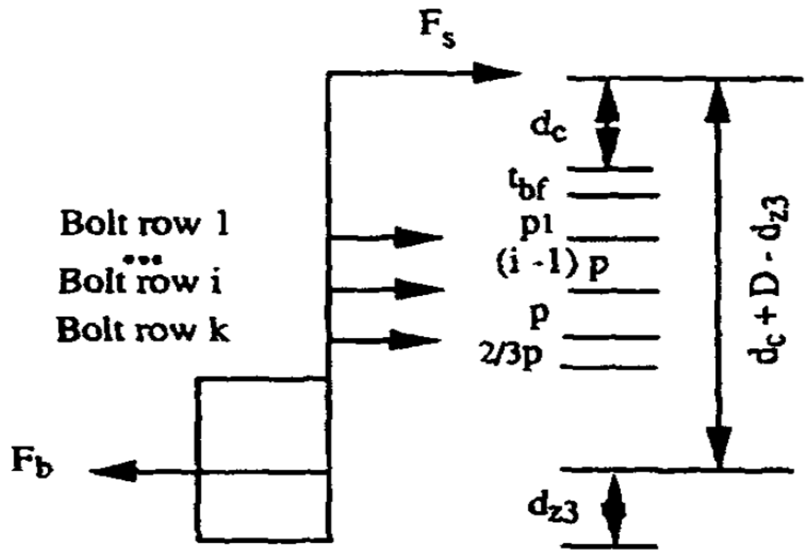

Figure 2.6 Neutral axis within beam's web below top row of bolts (Xiao *et al*., 1994)

In this case the bolt rows in tension zone will all be assumed to yield except for the lowest row. This assumption has been carefully examined by looking in detail at results from several tests and analyses.

Assuming K rows of bolts to be in tension, a region extending to two-thirds of the vertical pitch directly below the lowest row of bolts is considered to be in tension. The internal force equilibrium yields the condition:

$$K = \frac{p_y t_{bf} f_1 - F_s + p_y t_{bw}\left(D - p_1 - t_{bf} + \frac{1}{3}p\right)}{2F_t + p_y t_{bw} p} \qquad (2.1)$$

where p_y is the yield strength, F_s is the minimum of {capacity of stud, capacity of rebar}, D is the depth of the steel beam, p_1 is the distance from top bolt row to top surface of the steel beam, p is the bolt pitch, F_t is the bolt tensile strength, and f_1 is the width of the beam flange.

If K is smaller than 1, one row of the bolt will be treated as being in tension. A bolt row will reach yield when K is 1. If K is greater than 1, the tensile bolt row number which has been obtained from Eq. 2.1 will be a real number; where the integer part *i* represent the rows of bolts which have yielded, and the decimal part *j* represents the stress factor for the rows of bolts which have not yielded and is adjacent to the neutral axis. The total rows of bolts in the tension zone will be *i+j*.

$$K = i+j \tag{2.2}$$

The distance from the bottom surface of the steel beam to the centroid of compression can be defined as:

$$d_{z3} = \frac{t_{bw}\left[\left(D - p_1 - ip - \frac{2}{3}p\right)^2 - t_{bf}{}^2\right] + f_1 t_{bf}{}^2}{2\left[\left(D - p_1 - ip - \frac{2}{3}p - t_{bf}\right)t_{bw} + f_1 t_{bf}\right]} \tag{2.3}$$

Thus, the distance between the center of reinforcement and the centroid of the compressive area becomes:

$$d_c + D - d_{z3} \tag{2.4}$$

The contribution of the reinforcement bars to the connection's moment capacity is obtained by:

$$M_s = F_s\left(d_c + D - d_{z3}\right) \tag{2.5}$$

All the bolt rows in the tension region will also contribute to the moment capacity as follows:

$$M_b = M_1 + M_2 + ... + M_i + M_{i+1} \tag{2.6}$$

and

$$M_i = 2F_t\left(D - p_1 - p - \frac{2}{3}p - d_{z3}\right) \tag{2.7}$$

The moment capacity for a composite connection can be derived as:

$$M_u = M_s + M_b \tag{2.8}$$

Xiao *et al.* (1994) have proposed a method similar to the SCI method to calculate the available rotation capacity of the composite connections. By calculating the extension of the rebar, the rotation capacity was defined as:

$$\Phi_U = \left[\frac{\Delta L}{D + D_r}\right] \tag{2.9}$$

where D is the depth of the beam and D_r is the distance of the upper flange of the beam to the centre of the reinforcement.

The elongation of reinforcement (ΔL) consists of two parts: the deformation of the reinforcement in the plastic zone (L_1) and the deformation of reinforcement in the remaining elastic zone (L_2). Xiao *et al.* (1994) concluded that the elongation of the reinforcement in the elastic zone had no effect on the rotation capacity and therefore could be neglected. The elongation in the plastic zone was calculated as:

$$L_1 = \varepsilon\left[P_1 + P + \frac{D}{2}\right] \tag{2.10}$$

where P_1 is the distance of the column flange to the first shear stud, P is the pitch of the shear studs, and ε is the plastic strain of reinforcement taken as 0.005.

Xiao *et al.* (1994) used the location of the neutral axis to determine the rotation capacity of composite connections. The rotation capacity also considers the slip of the shear studs. The rotation capacity was defined considering four different location of neutral axis:

1. Neutral axis in the concrete slab
2. Neutral axis in the top flange
3. Neutral axis between the top flange and the top bolt row
4. Neutral axis below the top bolt row

The model is similar to the one in Figure 2.7. Amongst these possibilities, the last one is the most likely one and hence is described in detail. The rotation capacity for the last case is given by:

$$\Phi_u = \left[\frac{L_1}{d_c + p_1 + ip + \frac{2}{3}p} + \frac{L_2}{p_1 + ip + \frac{2}{3}p} \right] \tag{2.11}$$

where p is the bolt pitch, p_1 is the distance of the top bolt row from the top flange, d_c is the depth of the concrete slab, and i is the number of tension bolts that yielded and is given by the integer part of the following expression:

$$i = \text{integer part of} \left[\frac{p_y t_{bf} f_1 - F_s + p_y t_{bw}\left(D - p_1 - t_{bf} + \frac{1}{3}p \right)}{2F_t + p_y t_{bw} p} \right] \tag{2.12}$$

$$F_t = P_t A_t - Q_t \tag{2.13}$$

where P_t is the allowable bolt tensile stress from BS5950, A_t is the tensile area of the bolt, and Q_t is the prying force.

$$L_2 = \frac{F_s}{N.K} \tag{2.14}$$

where *N* is the number of shear studs and *K* is the secant stiffness of a shear stud, taken as 30 *kN/mm*.

The main drawback of the above formula is that the depth considered for the calculation of the rotation capacity becomes larger than the depth of the beam and sometimes greater than the combined beam and slab depth. This depth means that the beam is rotating without even having any physical contact with the column at the level of its bottom flange.

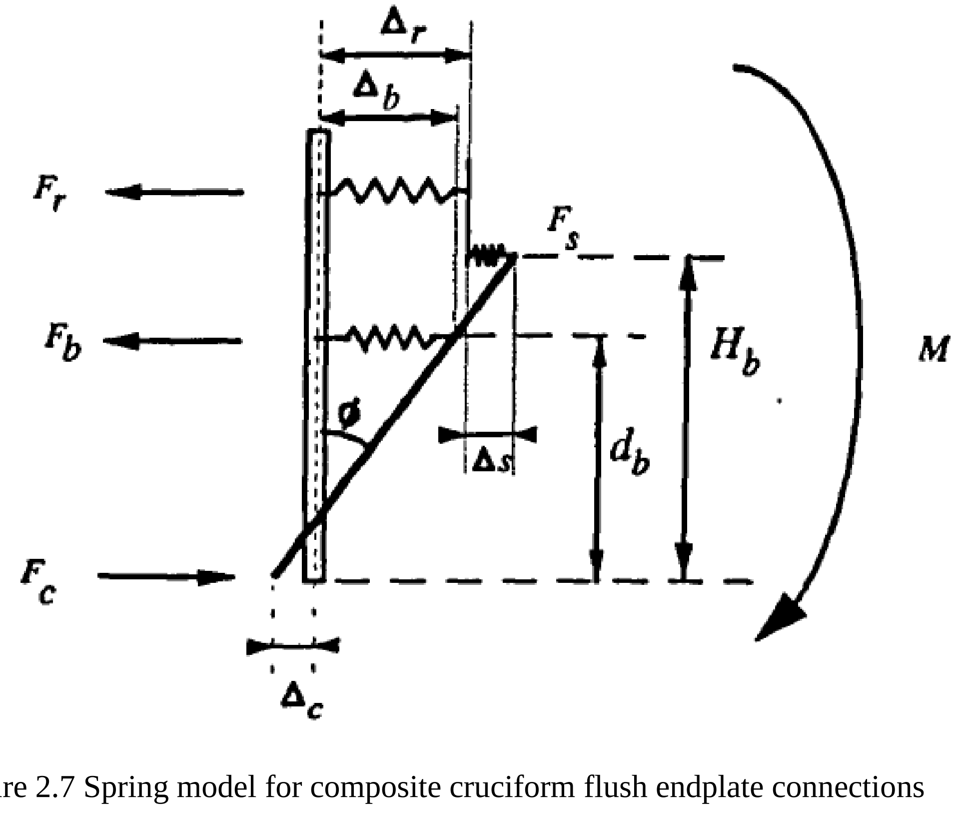

Figure 2.7 Spring model for composite cruciform flush endplate connections

2.5 FIBER REINFORCED POLYMER (FRP)

The use of FRP composites in strengthening reinforced concrete structures has been of great interest for civil engineers in recent years. Many researchers have strengthened different reinforced concrete members such as beams, columns and slabs with FRP laminates. Parvin and Granata (1998), Mosallam (2000) and Gergely *et al*. (2000) conducted some experimental and numerical studies on the subject of strengthening RC joints with FRP laminates. They pointed out the increase in the strength of joints and decrease in the ultimate rotation of the joints as a result of FRP strengthening of RC connections.

Application and demonstration projects of CFRP EBR (Externally Bonded Reinforced) started in the late 1980's throughout early 1990's. The use of carbon fiber for structural application in Europe was first studied at the Swiss Federal Testing Laboratories (EMPA). One of the first application considered which has proved to be commercially successful was the use of the CFRP plates as externally bonded reinforcement. The CFRP plates are much thinner than its steel counterpart, which allow lap joints to be made between different elements. The reduced eccentricity of the plate also reduces the tendency for peeling failure.

Carbon fiber sheets have been developed primarily in Japan and used for seismic retrofitting of existing RC structures. More than 1000 strengthening projects have been performed in a manner similar to the bonded steel plates. Currently, many grades of carbon fiber sheets are available, offering elastic modulus values from 230 to 640 kN/mm^2. Moreover, the carbon fiber can be aligned and woven in uni-directional and bi-directional ways to produce a fine mesh sheet of fiber. Thus, the designers have freedom of design when considering structural strengthening with CFRP sheets. CFRP sheets are easy to handle and install and also can be used in a variety of applications. They are ideal for complex shapes where strengthening is required.

Experimental studies involving bonded CFRP to reinforced concrete beams has been performed by Meier *et al*. since 1985 at the Swiss Laboratories for Materials

Testing and Research. This program envisioned the replacement of steel plates with FRP laminates for repairing and strengthening reinforced concrete beams. The examining of the strength and stiffness of beams with unidirectional CFRP plates was the primary focus of their research (Meier *et al*., 1985).

The first full-scale FRP repaired beam test conducted in the United States was at the University of Arizona (Saadatmanesh and Ehsani 1991) and using glass fiber reinforced polymer (GFRP). The tests consisted of six large concrete beams; five rectangle cross-sections (8"x18") and one T-beam (3"x24" flange, 8"x18" web). All the specimens were 192" long and tested as a simple span in four point loading. The steel reinforcement ratios, shear reinforcement, and cambering were varied in the six beams. However, the externally applied GFRP was identical for each beam (1/4"x10"x168"). The research concluded that adding GFRP plates improved the strength and stiffness of the specimens. The tests showed that the GFRP sheets carried a portion of the tensile force which decreased the stress in the steel reinforcement. This was particularly evident with the smaller steel reinforcement ratios.

2.6 NUMERICAL MODELING

Although the experimental measurements of strain and displacements with increasing load provide valuable insight into the problem, in many cases important local effects cannot be measured at all or cannot be measured with the necessary accuracy. This is due to the fact that the necessary measuring process is either impractical or is too expensive. Numerical studies thus provide a low cost-effectiveness ratio. Also the number of geometric and mechanical parameters which can reasonably be expected to influence the connection behavior is significant. In such cases numerical modeling is a very effective method for including more variables that could be contained in the limited scope of an experimental program. The most suitable tool available at present for studying such a complicated problem is the Finite Element Method (FEM). The FEM acts as a link between the experimental tests and the mechanical and analytical modeling.

The first numerical study on the composite connections was undertaken by Leon and Lin (1986). They used a general purpose FE software ADINA to model the connection. In their model, concrete was considered to have no tensile resistance. They modeled a connection tested by Leon (1986).

CHAPTER III

RESEARCH METHODOLOGY

3.1 INTRODUCTION

Finite element analysis is one of the several numerical methods that can be used to solve complex problems and is the dominant method used today. As the name implies, it takes a complex problem and breaks it down into a finite number of simple problems. Theoretically, a continuous structure has an infinite number of simple problems However, finite element analysis approximates the behavior of a continuous structure by analyzing a finite number of simple problems. Each element in a finite element analysis is one of these simple problems. In a finite element model, each element will have a fixed number of nodes that define the element boundaries to which loads and boundary conditions can be applied. The behavior of the variables in each type of element is defined by a suitable shape function. From the shape function, for each element, the stiffness matrix is developed. Then the stiffness matrices are assembled into the global stiffness matrix. The applied load is arranged in a matrix known as the load matrix. Using the basic equation: $[F] = \sum [K][d]$ the displacement at every nodal point is calculated. From the displacements, element stresses and nodal stresses are calculated. The finer the mesh is, the closer we can approximate the geometry of the structure, the load application, as well as the stress and strain gradients. However, there is a tradeoff: the finer the mesh is, the more computational power is needed to solve the complex problem. The strategy of optimizing the mesh size can greatly reduce an analyst's time without compromising on the quality of analysis results.

3.2 NON-LINEAR FINITE ELEMENT MODEL

In a linear analysis, the behavior of the structure is assumed to be reversible (i.e., the body returns to its original un-deformed state upon the removal of the applied load). However, in cases of a buckling, failure analysis, or the large deformation including those beyond the elastic limit, it is not possible to superimpose the solution from several load cases to obtain the solution for a higher load case. In such cases non-linear finite element analysis is required. In practice four types of non-linearity can be identified:

- Material non-linearity (non-linear stress-strain relation but linear strain displacement relation). An example of this is the elastic-plastic behavior in materials.

- Geometric non-linearity (non-linear strain-displacement relation but linear stress-strain relation). An example of this is elastic post buckling of structures.

- Combined material and Geometric non-linearity. An example of this is the deformation of rubber-like materials.

- Boundary non-linearity (when the deformations and stresses at contacting bodies are not linearly dependent on the applied load). This is due to the fact that the extent of the contact area changes with the applied load.

Note that semi-rigid composite connections possess material, geometric, and boundary nonlinearity.

3.2.1 The stiffness matrix in non-linear problems

In linear problems, the overall stiffness matrix [K] is a function of geometry and material properties, not the boundary conditions or the applied load. Therefore, the element stiffness matrix $[K_e]$ remains constant for linear problems and is calculated as follows:

$$[K_e] = \int_v [B]^T [D][B] \mathrm{d}v \tag{3.1}$$

where $[D]$ is the material property matrix and $[B]$ is the shape function matrix.

In non-linear problems, the overall stiffness matrix [K] is a function of the current state of stress and strain. Therefore, $[K_e]$ must be updated to take into account for the change in material properties and/or the geometry with the current stress and strain. For nonlinear problems, $[K_e]$ can be written as:

$$[K_e] = f(F,u) \tag{3.2}$$

where F is the external forces and u is the displacement.

Figure 3.1 shows the basic effect of variation of the stiffness matrix in linear and nonlinear problems.

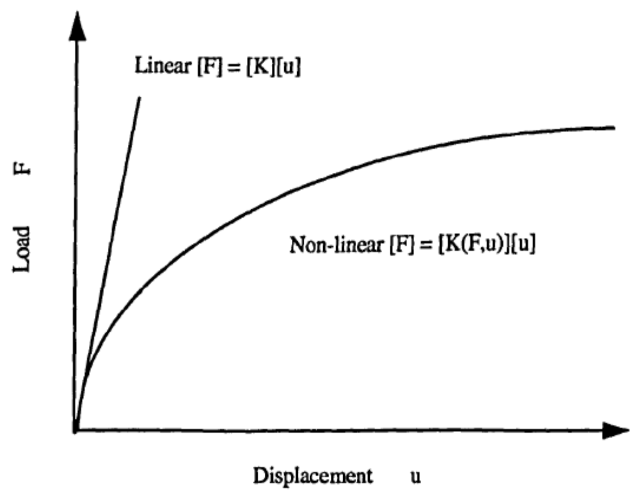

Figure 3.1 Stiffness matrix in nonlinear problems

3.2.2 Numerical procedure in non-linear problems

ANSYS employs the "Newton-Raphson" approach to solve nonlinear problems. In this approach, the load is subdivided into a series of load increments. The load increments can be applied over several load steps. Figure 3.2 illustrates the use of Newton-Raphson equilibrium iterations in a single DOF nonlinear analysis.

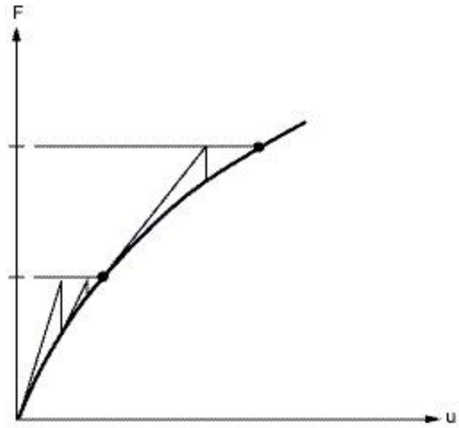

Figure 3.2 Newton-Raphson Approach
Source: ANSYS Help

Before each solution, the Newton-Raphson method evaluates the out-of-balance load vector which is the difference between the restoring forces (the loads corresponding to the element stresses) and the applied loads. The program then performs a linear solution using the out-of-balance loads and checks for convergence. If convergence criteria are not satisfied, the out-of-balance load vector is reevaluated, the stiffness matrix is updated and a new solution is obtained. This iterative procedure continues until the problem converges.

A number of convergence-enhancement and recovery features such as line search, automatic load stepping, and bisection can be activated to help the problem to converge. If convergence cannot be achieved, the program attempts to solve with a smaller load increment.

In some nonlinear static analyses, if one uses the Newton-Raphson method alone, the tangent stiffness matrix may become singular (or non-unique) causing severe convergence difficulties. Such occurrences include nonlinear buckling analyses in which the structure either collapses completely or "snaps through" to another stable configuration. For such situations, one can activate an alternative iteration scheme (the arc-length method) to help avoiding bifurcation points and track unloading.

The arc-length method causes the Newton-Raphson equilibrium iterations to converge along an arc, therefore, often preventing divergence even when the slope of the load vs. deflection curve becomes zero or negative. Figure 3.3 schematically shows the iteration method.

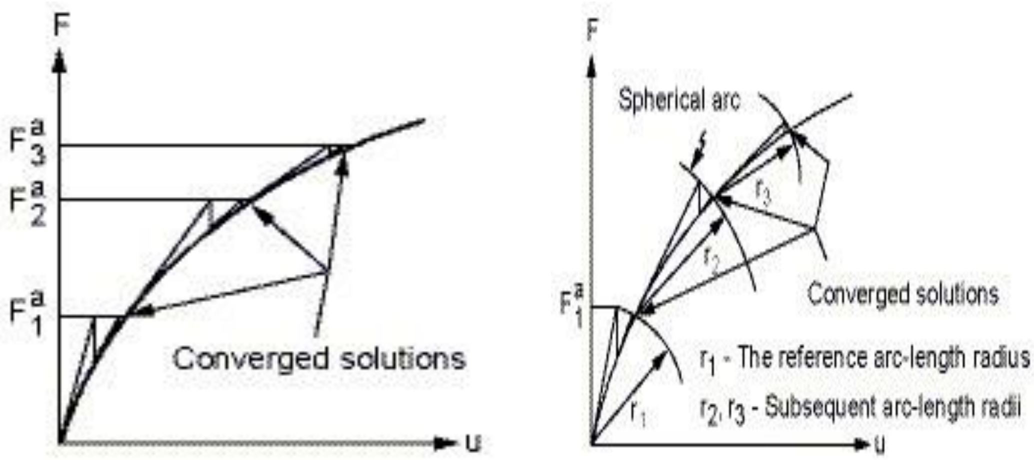

Figure 3.3 Traditional Newton-Raphson method vs. Arc-Length method
Source: ANSYS Help

To summarize, a nonlinear analysis is organized into three levels of operation:

- The "top" level consists of the load steps that you define explicitly over a "time" span. Loads are assumed to vary linearly within load steps.

- Within each load step, one can direct the program to perform several solutions (sub-steps or time steps) to apply the load gradually.

- At each sub-step, the program will perform a number of equilibrium iterations to obtain a converged solution.

Figure 3.4 shows a typical load history for a nonlinear analysis.

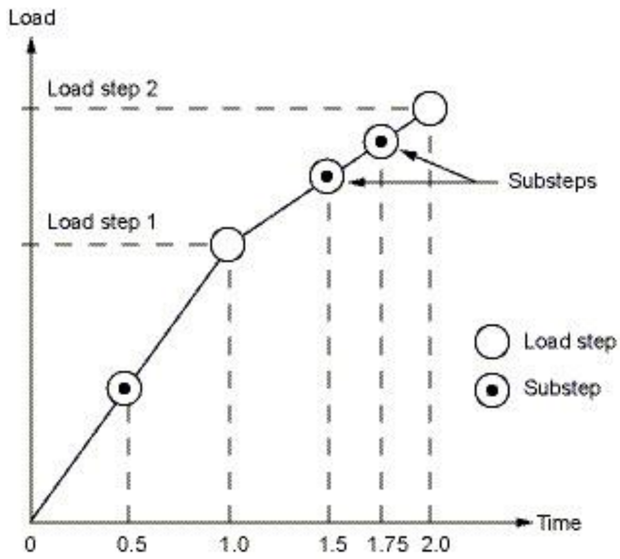

Figure 3.4 Load Steps, Sub-steps, and Time
Source: ANSYS Help

The ANSYS program gives a number of choices when designated a convergence criteria: the convergence checking can be based on forces, moments, displacements (or rotations) or any combination of these items. Additionally, each item can have a different convergence tolerance value. For multiple-degree-of-freedom problems, one also have a choice of convergence norms.

The user should mostly employ a force-based (and when applicable, moment-based) convergence tolerance. The displacement-based (and when applicable, rotation-based) convergence checking can be added, if desired, but should usually not be used alone.

3.3 MODELING

Modeling involves creating a geometric representation of a structure and defining its characteristic behavior in terms of its physical properties such as material, loading, and support.

3.4 GEOMETRY

All engineering simulation starts with geometry to represent the design. This could be a solid component for a structural analysis, the air volume for a fluid, or an electromagnetic study. The geometry can be produced in a computer-aided design (CAD) system or built from scratch. The ANSYS Design Modeler software is the gateway to geometry handling for analysis with software from ANSYS.

ANSYS Design Modeler technology also provides powerful tools for construction of geometry from the scratch. A complex model can be produced using familiar solid modeling operations. Built on the Parasolid kernel, the geometry engine is robust and conforms to industry standards. The two-dimensional sketches can be extruded into 3-D solids and then modified with Boolean operations. A construction history is recorded during the creation of the geometry allowing the user to make changes and then update the design.

Two 305*165*UB40 of 1.6 *m* in length and one 203*203*UC52 were connected to form the cruciform arrangement. The beams were connected to the column flanges by means of partial-depth endplates (150*190*10 *mm*) and two rows of M20 Grade 8.8 bolt. A 120 *mm* deep slap with RMF CF46 profiled metal decking used. The slab reinforcement ratio is 0.8 % (see Figure 3.5).

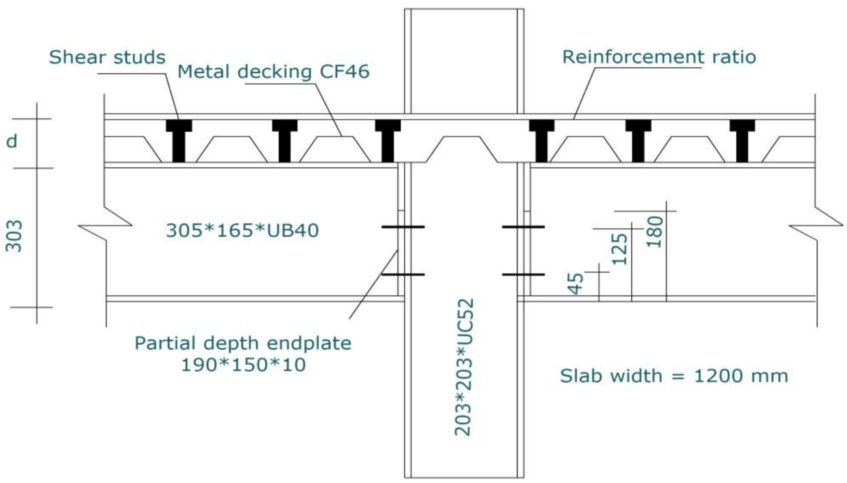

Figure 3.5 Cruciform arrangement of partial depth endplate composite connection (reproduced from Xiao *et al*., 1994: SCJ10)

3.5 MESHING

Points, lines, surfaces, and volumes allow the exact smooth geometry of the problem to be defined or imported. However, to solve the problem, the model must be broken down into nodes and elements. This process is known as meshing and the collective term for all elements and nodes, once created, is the mesh. The special attributes, (mesh attributes) can be created and assigned to geometry. They define the type and number of nodes and elements that will be used to represent each part of the geometry.

Meshing is an integral part of the computer-aided engineering simulation process. The mesh influences the accuracy, convergence, and the speed of the solution. Furthermore, the time it takes to create and mesh a model is often a significant portion of the time it takes to get results from a computer-aided engineering (CAE) solution. Therefore, the better and more automated the meshing tools are, the better the solution is.

Once the best design is found, the meshing technologies from ANSYS provide the flexibility to produce meshes that range in complexity from pure hex to highly detailed hybrid. A user can put the right mesh in the right place and ensure that a simulation will accurately validate the physical model.

ANSYS has a range of meshing tools that cater to nearly all physics. While the meshing technologies were developed to meet the needs in a specific area; solid, fluid, electromagnetic, shell, 2-D or beam models, accessing to these technologies is available across all physics.

With automatic contact detection and setup, a user requires little training to perform sophisticated analysis. In addition, users can generate pure hex meshes using one of several mesh methods depending on the type of the model and whether the user wants a pure hex or hex-dominant mesh. The finite element mesh scheme used for shear studs in this study can be seen in Figure 3.6.

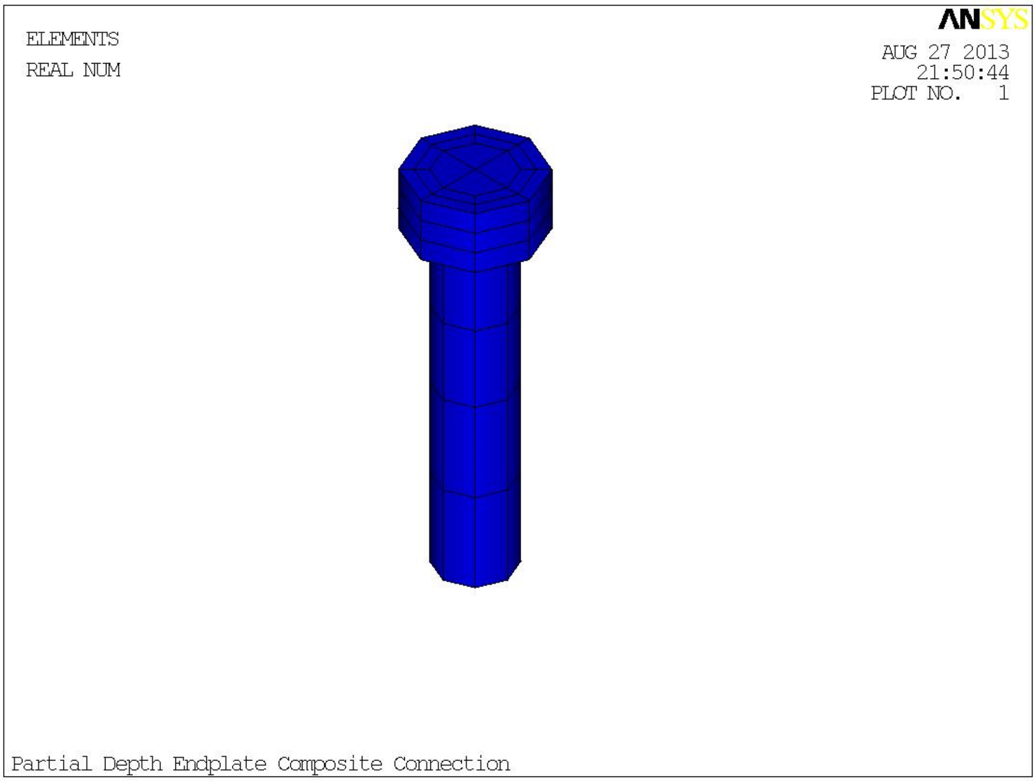

Figure 3.6 Shear stud meshing

The choice of the right element is another important step which should be specially taken into account. The Metal deck and beam were modeled with eight-nodded thin shell elements (SHELL281) and the concrete slab with solid elements (SOLID185). The einforcements were modeled using the link element (LINK8) and shear connectors idealized by 20-nodded solid elements (SOLID95). The eight-node solid elements (SOLID45) were used to model column, endplate, and bolts. Layered 8-node solid elements (SOLID46) were used to model CFRP laminate. The interaction between the metal deck and the steel beams is not fully bonded. Due to this reason, a surface to surface contact element was used as an interface element between the metal deck and steel beam to prevent any penetration of steel decking into the steel beam. To model this behavior, the surface-to-surface contact elements (CONTA174 and TARGE170) were superimposed on the surfaces of the solid or shell elements that form the interface. Each of these “contact pairs” is also capable of representing the slide between the two surfaces activated by defining a friction coefficient (ANSYS 2009). The complex interface between the endplate and the column flange, the shear studs and concrete, and the column flange and concrete were also defined by surface-to-surface contact model. The coefficient of friction was assumed as 0.45 in this study. Longitudinal reinforcement bar arrangement can be seen in Figure 3.7.

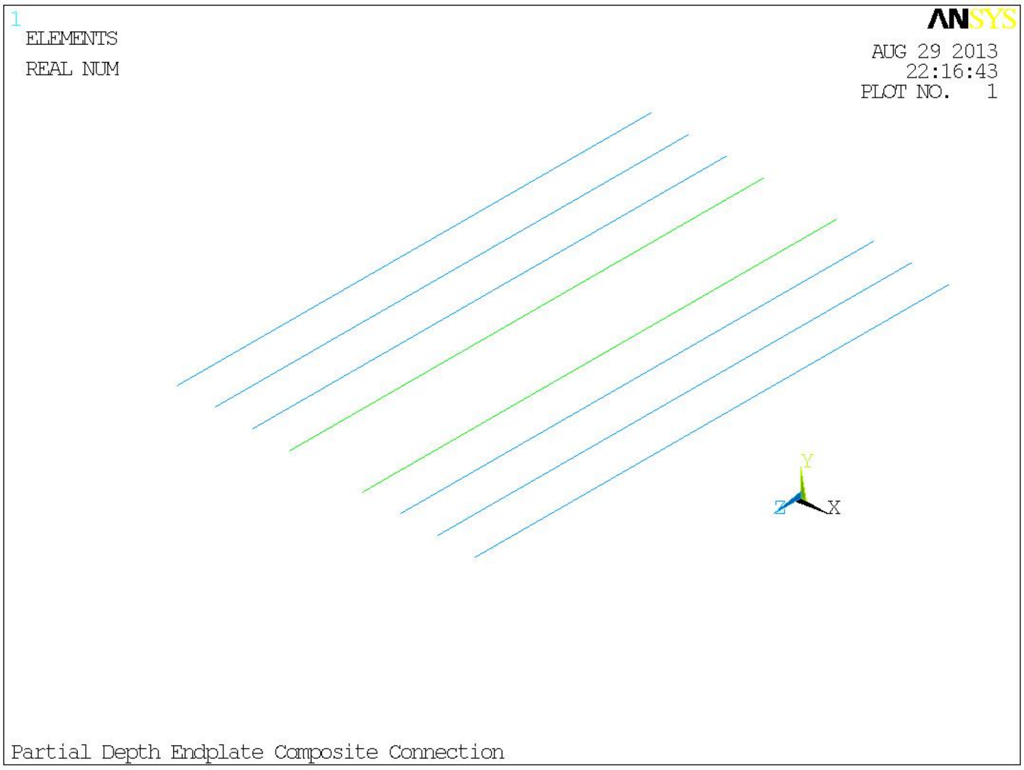

Figure 3.7 Longitudinal reinforcement bars position for SCJ10 (2T12 & 6T10)

3.6 BOUNDARY CONDITION

Since the advantage of symmetry was used to reduce the problem size, it was essential to address the problem with proper boundary conditions. To define the support condition or to establish symmetry, appropriate restraints on nodes or node sets are required. The nodes can be restrained for any/all displacements or any/all rotations, or for both. In view of the symmetry about two axes of cross-section, the concrete-steel composite connections are modeled with half the length. This results in a significant reduction of the computational time and computer disc space requirement. All forces and rotations are 0 in Z direction for the line of symmetry. Figure 3.8 shows the boundary conditions of the developed model in ANSYS.

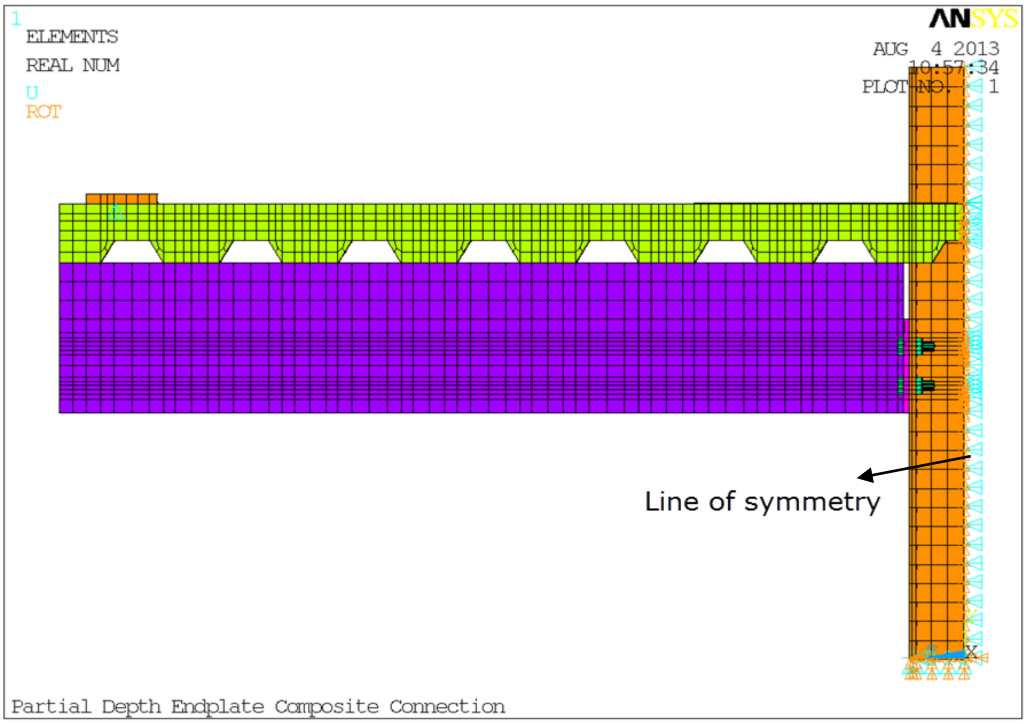

Figure 3.8 Boundary conditions

3.7 LOADING

In linear analysis, superposition is used to calculate the results for combination load cases, but in non-linear analysis this may not be valid. The results for a combination load case are obtained in non-linear analysis by adding up all the component load cases and then performing the analysis for the combined loads. It would be a wasted effort to analyze a load case which cannot exist on its own. Two loads of the same magnitude are applied symmetrically to each cantilever at 1.5 *m* from the column flange.

ANSYS uses an incremental solution procedure to obtain a solution to a nonlinear analysis. In this study, the total external displacement within some load steps, depending on span length, were applied in increments over a certain number of substeps. As described earlier in this chapter, ANSYS uses a Newton-Raphson iterative procedure to solve each substep. The number of substeps for each load step should be specified, since this number controls the size of the initial displacement increment applied in the first substep of each load step. ANSYS automatically determines the size of the displacement increment for each subsequent substep in a load step. The size of the displacement increment for these subsequent substeps should be controlled by specifying the maximum and minimum number of substeps. If the number of substeps is defined, the maximum and minimum number of substeps to be the same, then ANSYS uses a constant displacement increment for all substeps within the load step.

3.8 MATERIAL PROPERTIES

For the material properties, ANSYS requires the input of the elastic modulus, yield stress, and Poisson’s ratio of the steel and elastic modulus, compressive strength, and Poisson’s ratio of concrete. In this study, Poisson’s ratio of 0.3 and 0.2 were used for steel and concrete, respectively. The multi-linear strain hardening stress-strain curves were used for steel and concrete.

To model the behavior of reinforced concrete in a composite slab, SOLID185 was chosen to represent the concrete. The element is defined by eight nodes having three degrees of freedom at each node. The element has plasticity, hyper-elasticity, stress stiffening, creep, large deflection, and large strain capabilities. The stress-strain behavior of concrete is shown in Figure 3.9.

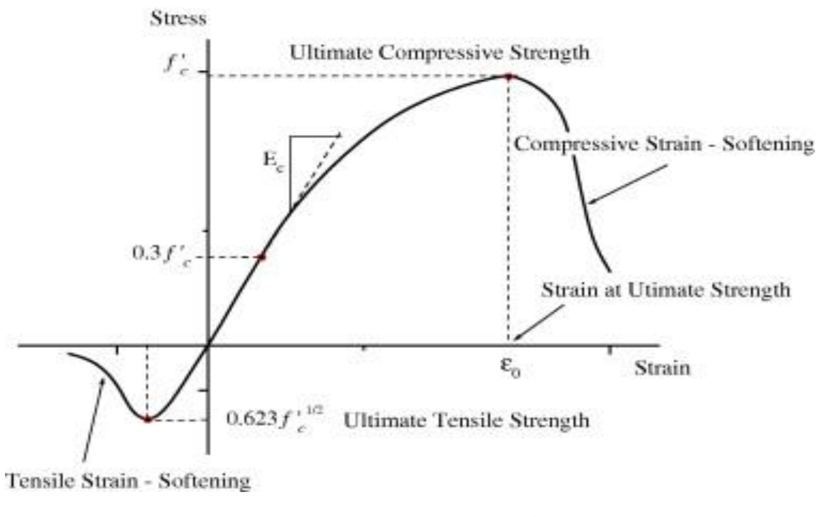

Figure 3.9 Typical stress-strain curve for concrete

The compressive stress f_c' is taken as 0.78 f_{cu} where f_{cu} is the cube compressive strength of the concrete. The relationship between ultimate concrete compressive and tensile strengths and modulus of elasticity are expressed as:

$$E_c = 4700\sqrt{f_c'} \tag{3.3}$$

$$f_r = 0.632\sqrt{f_c'} \tag{3.4}$$

For the ascending portion of Figure 3.9, the uniaxial stress-strain relationship for the concrete model was obtained using the following equations to compute the multilinear isotropic stress-strain curve for concrete.

$$f = \frac{E_c \in}{1 + (\frac{\in}{\in_0})^2} \tag{3.5}$$

$$\in_0 = 2\frac{f_C'}{E_c} \tag{3.6}$$

$$E_c = \frac{f}{\in} \tag{3.7}$$

where *f* is the stress at any strain and $\in_0$ is the strain at the ultimate compressive strength.

The shear stud and metal deck were modeled using a bilinear stress-strain curve with the BISO option in ANSYS. The bilinear stress-strain curve is capable of representing elastic-perfectly plastic material behavior with equal yield stresses in tension and compression as well as with the hardening option as can be seen in Figure 3.10.

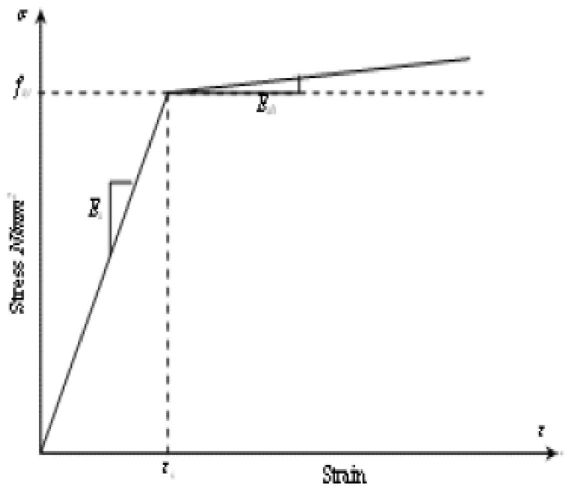

Figure 3.10 Stress-Strain curve for metal deck and shear studs

Steel reinforcement is modeled for nonlinear analysis as an elastic-plastic material with a strain hardening and yielding plateau beyond the elastic phase. It is assigned a three linear stress-strain law, symmetrical in tension and compression as shown in Figure 3.11.

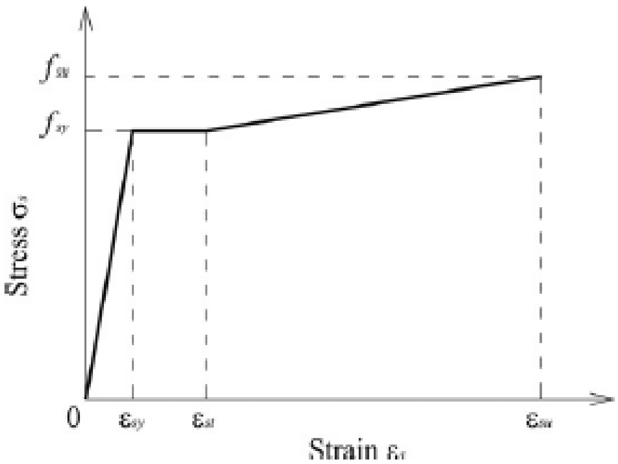

Figure 3.11 Stress-Strain curve for steel reinforcement bars

Other structural steel parts were modeled using a multilinear isotropic hardening. The stress-strain relation used by Gattesco *et al.* (1999) has been adopted. The use of a nonlinear curve will increase the degree of accuracy compared with a linear curve. The typical stress-strain curve for these parts is shown in Figure 3.12.

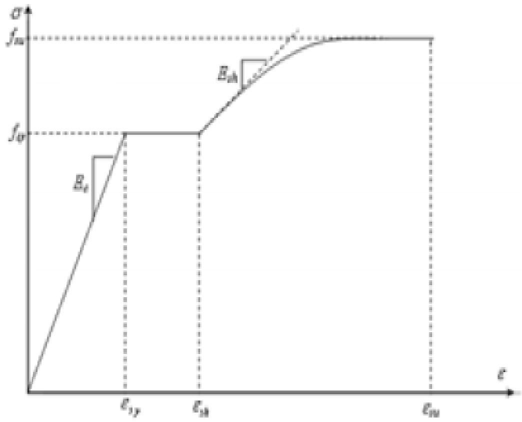

Figure 3.12 Multilinear stress-stain curve

The material properties for the composite connections are given in Table 3.1.

Table 3.1 Material properties for the composite connections

Material	Elastic Modulus (Mpa), E_s	Yield Stress (Mpa), f_y	Ultimate tensile stress (Mpa), f_y	compressive cube strength (Mpa), f_{cu}
Bar T10	190000	504	622	
Bar T12	190000	497	870	
A142Mesh	190000	657	705	
Metal deck	125400	350		
Column web	125400	317.66	457.91	
Column flange	125400	289.80	458.83	
Beam web	125400	342.24	466.69	
Beam flange	125400	295.33	473.85	
Shear stud	125400	300		
Bolt	125400	640		
Endplate	125400	289.8		
Bearing plate	125400	300		
Concrete	20324			18.7

In this research, a 3-D layered structural element SOLID 46 was used to model the CFRP laminate. The element allows up to 250 layers. The element has three degrees of freedom at each node: translation in x , y , z directions. The element is defined by eight nodes, layer thickness, layer material direction angles and orthotropic material properties. The geometry and coordinate system is shown in the Figure 3.13.

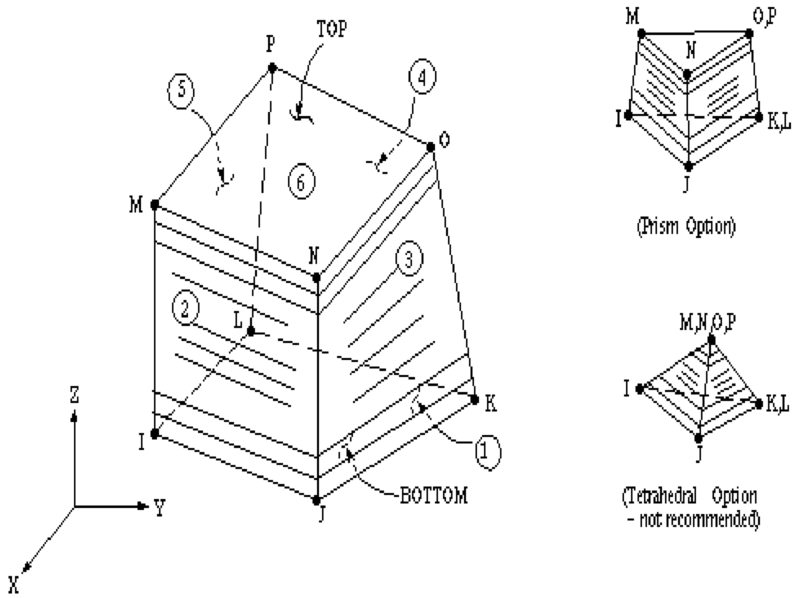

Figure 3.13 SOLID46 Element Geometry and Coordinate system
Source: ANSYS help

As defined by the element, the input data are the number of layers, the thickness of the layers, and the orientation of the fiber direction for each layer. The composites are orthotropic materials, therefore, nine different properties have to be input; the elastic modulus in three different directions (E_x , E_y , E_z), the shear modulus in three directions (G_{xy}, G_{yz}, G_{zx}), and the Poisson's ratio in three directions (ν_{xy}, ν_{yz}, ν_{zx}). Figure 3.14 gives the principal directions of the orthotropic material.

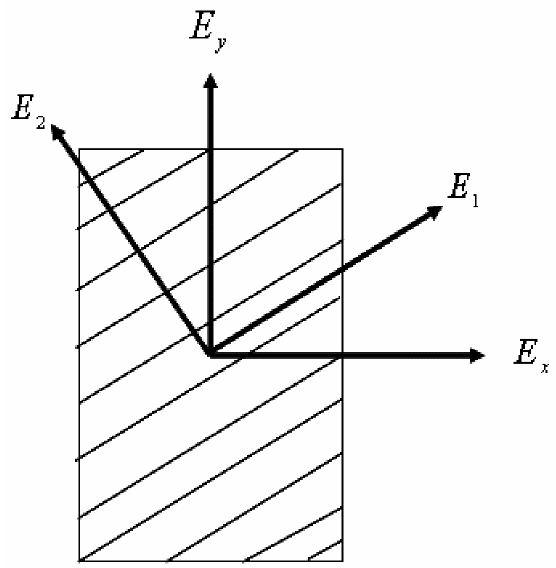

Figure 3.14 Principal directions of an orthotropic material

In the present research, the orientation of the fibers is along the hoop (0^0) direction. Therefore, they are considered as the unidirectional fibers. The principal directions of this unidirectional FRP composite can be seen in Figure 3.15.

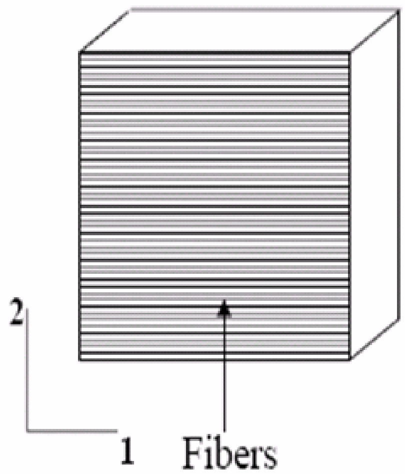

Figure 3.15 Principal directions of a unidirectional FRP composite

The CFRP laminates "MBRACE® laminate 460/1500" supplied by BASF were adopted for this study. It is an ultra-high modulus laminate with a nominal elastic modulus of 460 *GPa* and a nominal tensile strength of 1500 *MPa*. The elastic modulus and the tensile strength are around 2.3 and 4 times higher than those of the common steel products. The UHM CFRP plate has a fiber content of 71% and its measured thickness is 1.45 *mm*. The material properties for FRP composites are available in Table 3.2.

Table 3.2 Summary of material properties for CFRP composites

FRP composite	Tensile modulus (*MPa*)	Poisson's ratio	Tensile strength (*MPa*)	Elongation at break (%)	Thickness of laminate (*mm*)
MBRACE ® laminate 460/1500	478.730	0.36	1607	0.36	1.45

CHAPTER IV

RESULTS AND DISCUSSIONS

4.1 INTRODUCTION

In this chapter, comparisons are made between the FEM results. The key properties of the composite joint with respect to moment capacity, rotational stiffness, and rotation capacity will be discussed and compared.

Specimen SCJ10 tested by Xiao *et al.* (1994) at the University of Nottingham serves as the benchmark model for comparison with those finite element models with CFRP laminates. A direct comparison between the strengthened and un-strengthened composite connections can be made and the effect of having laminates can be studied. The moment-rotation curve will be plotted using the analytical results obtained from finite element analysis. The moment resistance and rotation capacity were obtained and then compared with the existing experimental result to prove the accuracy of the analytical result.

4.2 EXPERIMENTAL RESULT

The experimental result of the moment-rotation curve for specimen SCJ10 is shown in Figure 4.1. The experimental value of the moment resistance and rotation capacity were 147.8 *kN.m* and 16.5 *mRad*, respectively.

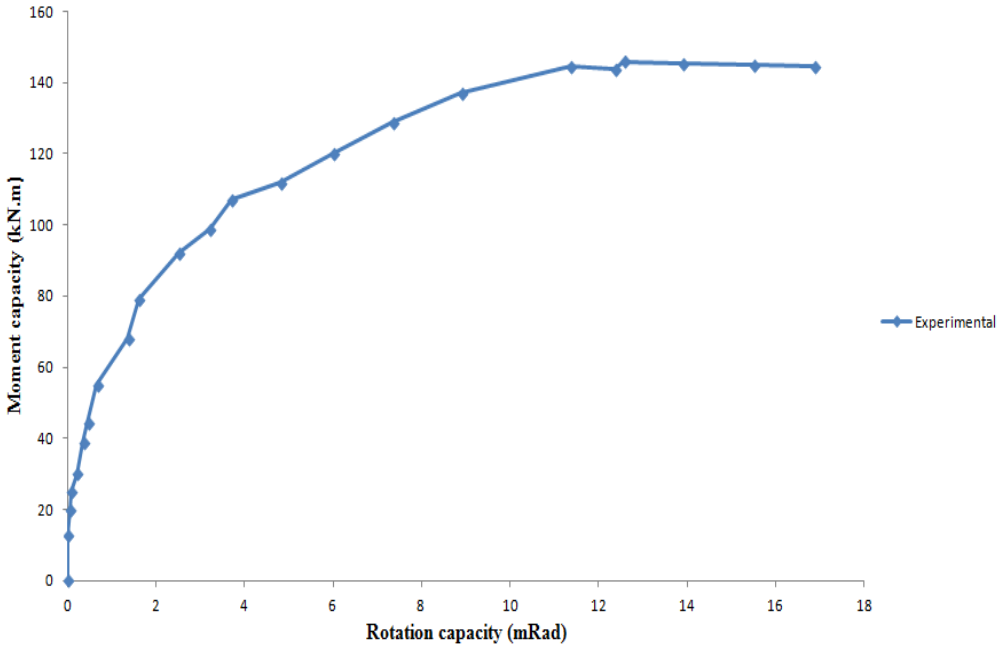

Figure 4.1 Experimental moment-rotation curve for SCJ10

4.3 VERIFICATION OF FINITE EEMENT MODEL

4.3.1 Convergence study

In finite element modeling, a finer mesh typically results in a more accurate solution. However, as a mesh is made finer, the computation time increases. For getting a mesh that satisfactorily balances between the accuracy and computing resources, the user needs to perform a mesh convergence study. Three steps of refining the meshes were done in this study for obtaining the proper mesh dimensions. These three steps with variable mesh dimensions for concrete slab is shown in Table 4.1. A finer meshing was used around shear studs due to the existence of stress concentrations in their vicinity as shown in Figure 4.2. From Figure 4.3, it can be seen that the moment-rotation curve for the finest mesh shows a good agreement with the experimental test (SCJ10) curve done by Xiao *et al.* (1994).

Table 4.1 Element meshing sizes

Mesh type	Concrete slab global mesh size (mm)
Coarse mesh	85
Finer mesh	35
Finest mesh	28

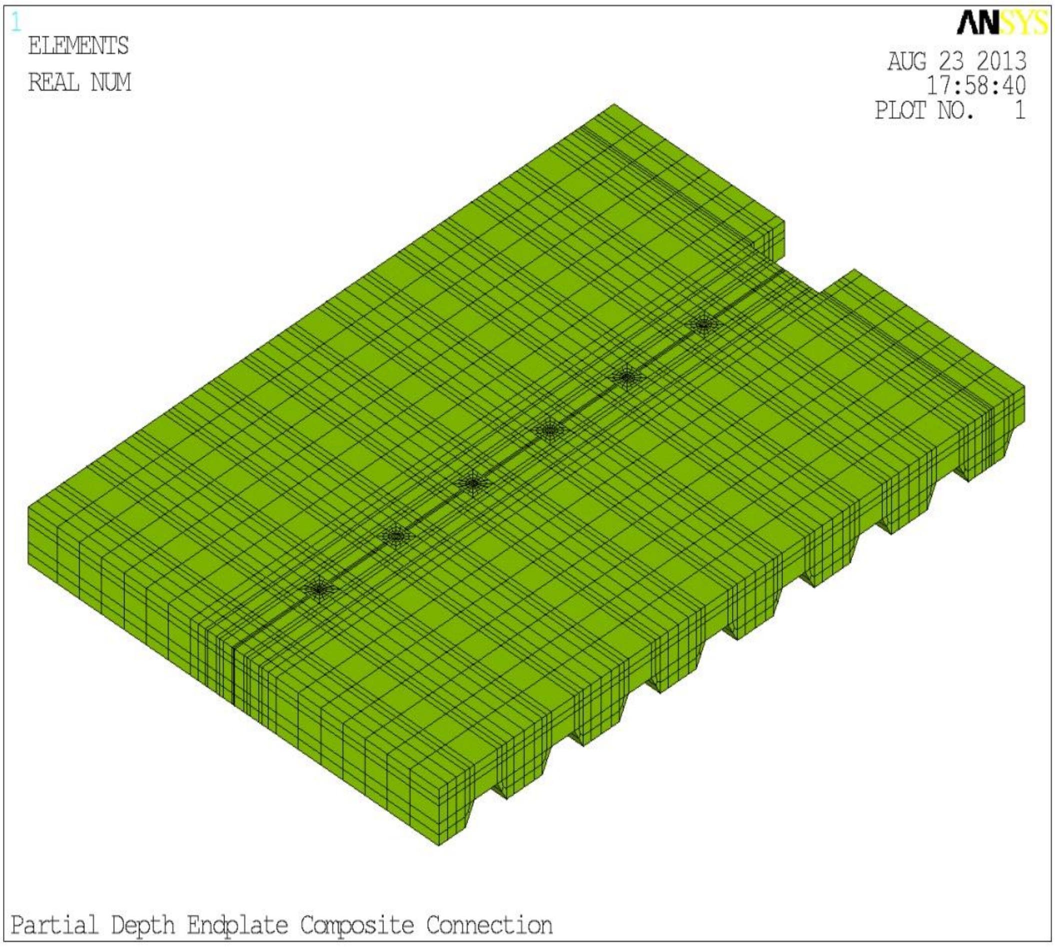

Figure 4.2 Concrete slab meshing (coarse mesh)

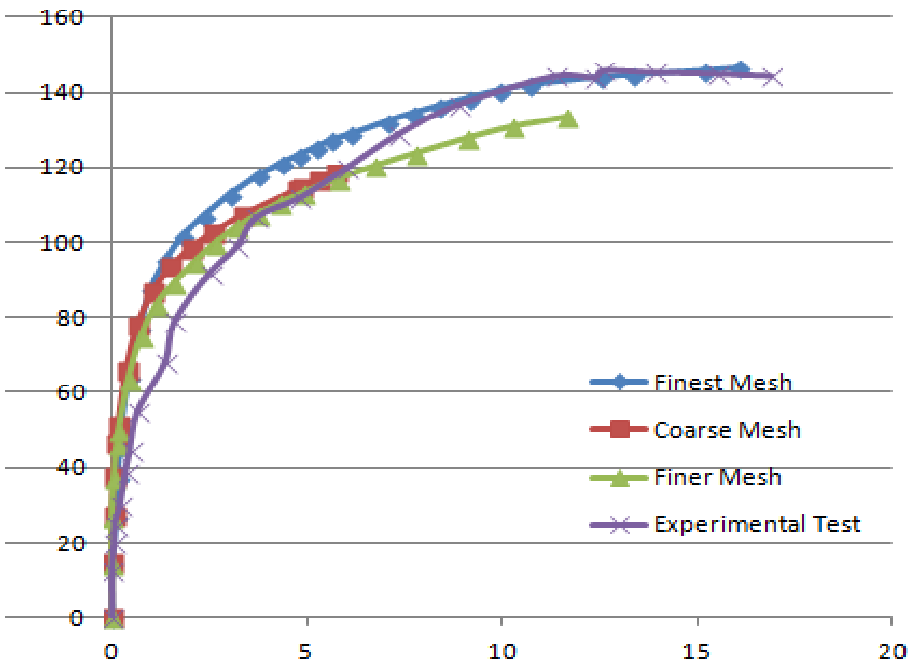

Figure 4.3 Convergence study

4.3.2 Comparisons of result between experimental test and FEM

The comparison of results is important to determine the accuracy of the finite element analysis of the connection. The comparisons are made in terms of the moment-rotation curve. The moment-rotation curve for specimen SCJ10 produced by laboratory test and ANSYS software is shown in Figure 4.4.

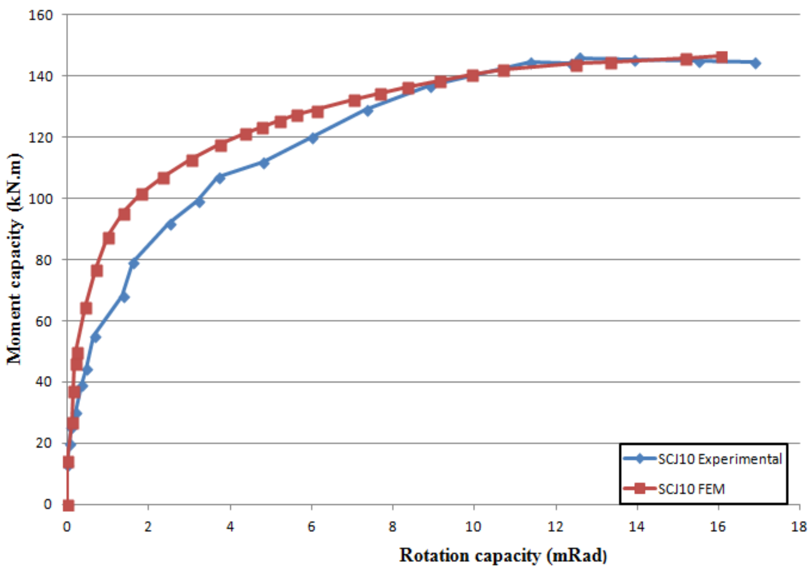

Figure 4.4 Comparisons between experimental and FEM results

By observing the two curves, it can be seen that both curves had similar trend. The connection initially behaves linearly at the first stage followed by nonlinear behavior at the second stage, where the connection gradually loses its stiffness with increasing rotation. The stress contour for the column and bolts up to the elastic stage is shown in Figure 4.5. The failure mode of the composite connection observed from FE analyses is column web buckling. This compares well with the test result (SCJ10) of Xiao *et al*. (1994).

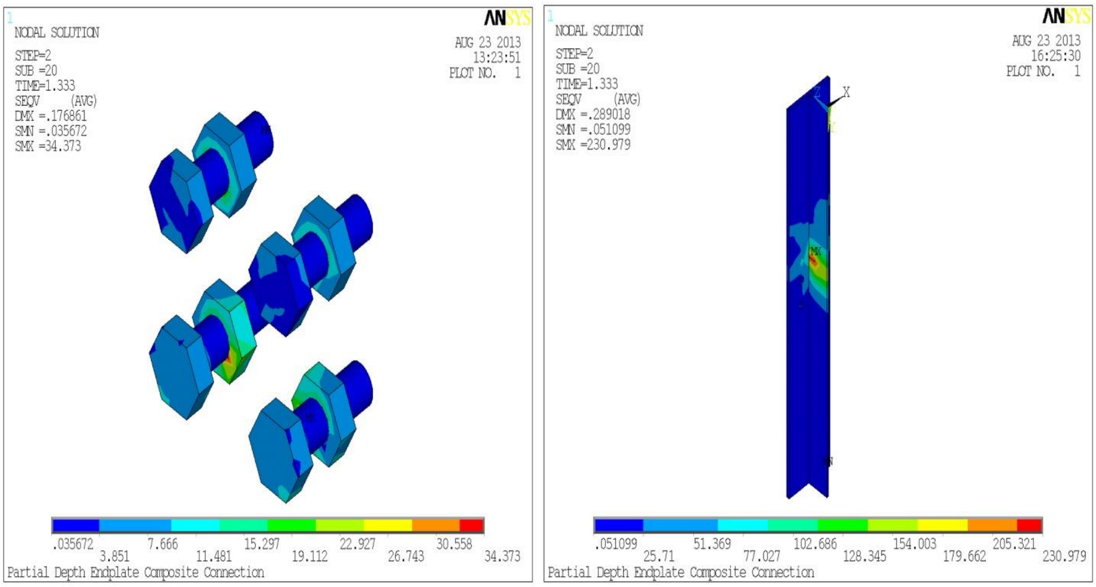

Figure 4.5 Stress contour up to the elastic stage for SCJ10

Figure 4.6 shows the stress contours in the ultimate moment capacity for SCJ10.

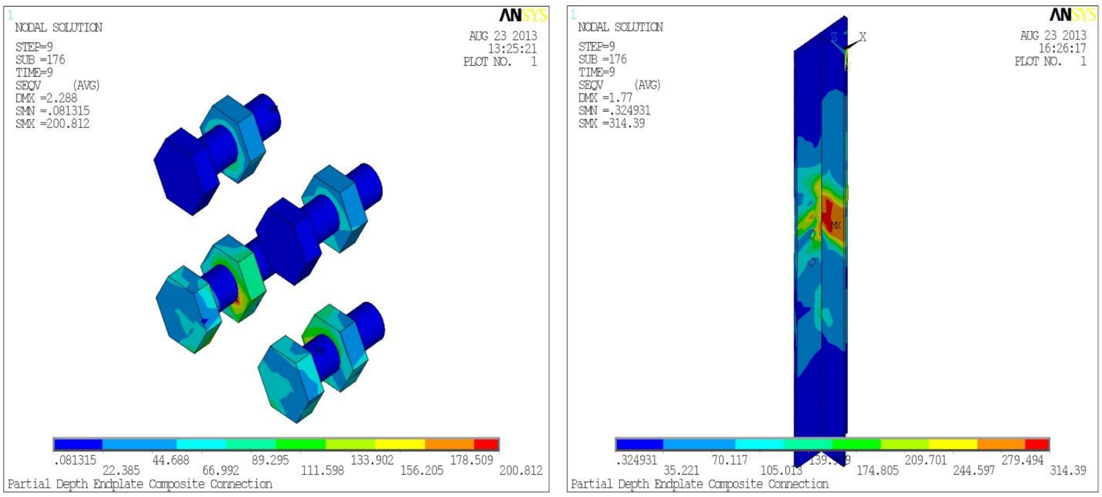

Figure 4.6 Stress contour for SCJ10 in ultimate moment capacity

The deformation of the partial depth endplate can be seen in Figure 4.7.

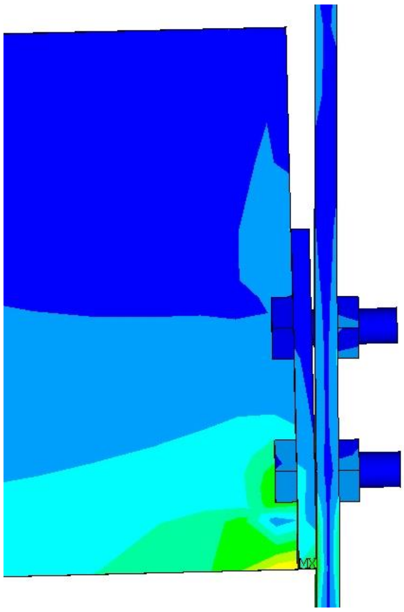

Figure 4.7 Deformation of partial depth endplate after FE simulation

4.4 CFRP REINFORCING

Several configurations of CFRP overlays are examined. A composite connection without a CFRP overlay is analyzed to serve as a reference point for comparisons of models using CFRP reinforcing.

CFRP sheet configurations in this study have a width of 30%, 45%, 50% and 60% of the slab width. The length of the CFRP sheets chosen for this study are 20%, 30% and 40% of the length of the composite slab. Figure 4.8 shows a model with a CFRP overlay applied to the tensile face of the connection. The overlay consists of CFRP laminate which has a width equal to 60% of the width of the composite slab. The overlay has a length equal to 40% of the length of the composite slab. The thickness of the laminate is 1.45 *mm*.

To investigate the effect of CFRP sheet configuration, five models with different width and length have been built in ANSYS 12.1. Table 4.2 shows the configurations of these models.

Table 4.2 CFRP laminates dimensions

Test	CFRP sheet width (% Slab width)	CFRP sheet length (% Slab length)	CFRP sheet thickness (mm)
CFRP1	30	30	1.45
CFRP2	45	30	1.45
CFRP3	50	20	1.45
CFRP4	60	30	1.45
CFRP5	60	40	1.45

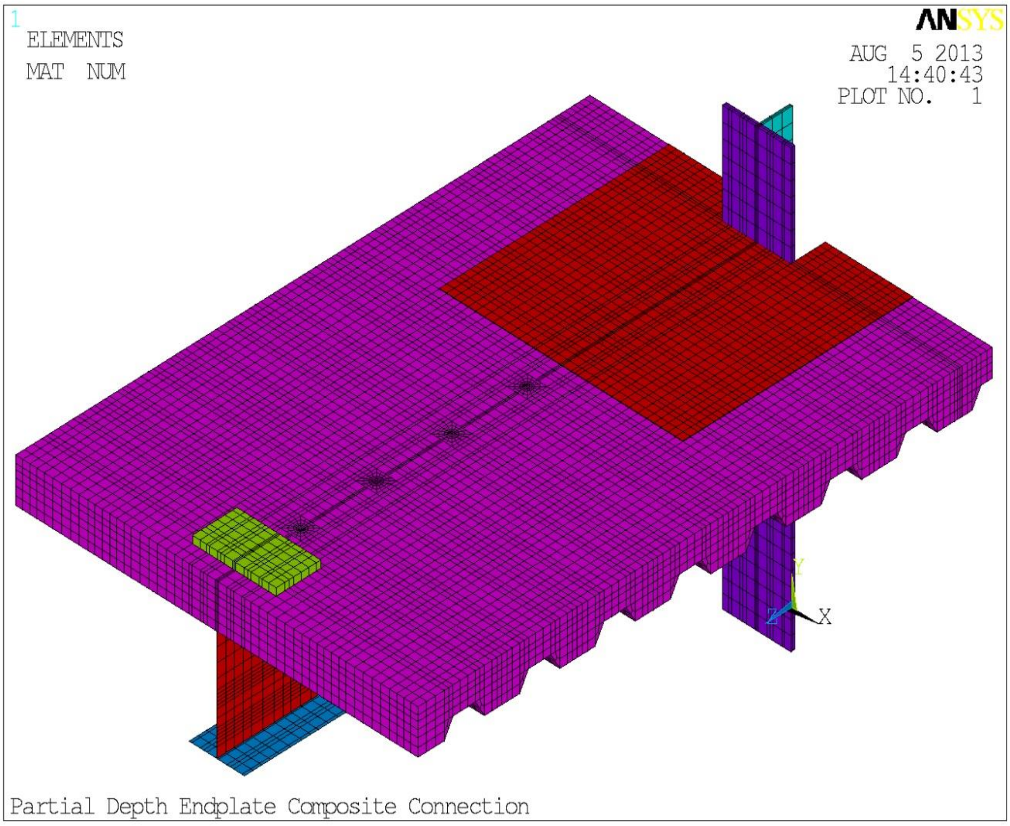

Figure 4.8 CFRP5 configuration in ANSYS (half of the experimental model)

Table 4.3 shows the moment resistance and the rotation capacity for un-strengthened and strengthened models with different CFRP laminate configurations. From the results, it can be seen that applying CFRP sheets to the tension face of the composite connection will increase the moment resistance and rotational stiffness of the connection.

Table 4.3 Results from un-strengthened and strengthened models

Test	Moment resistance (*kN.m*)	Rotation capacity (*mRad*)
Un-strengthened model (SCJ10)	146.469	16.045
CFRP1	150.342	6.91
CFRP2	158.097	6.747
CFRP3	149.08	7.573
CFRP4	162.627	6.631
CFRP5	175.919	7.264

The moment-rotation curves for these specimens are shown in Figure 4.9.

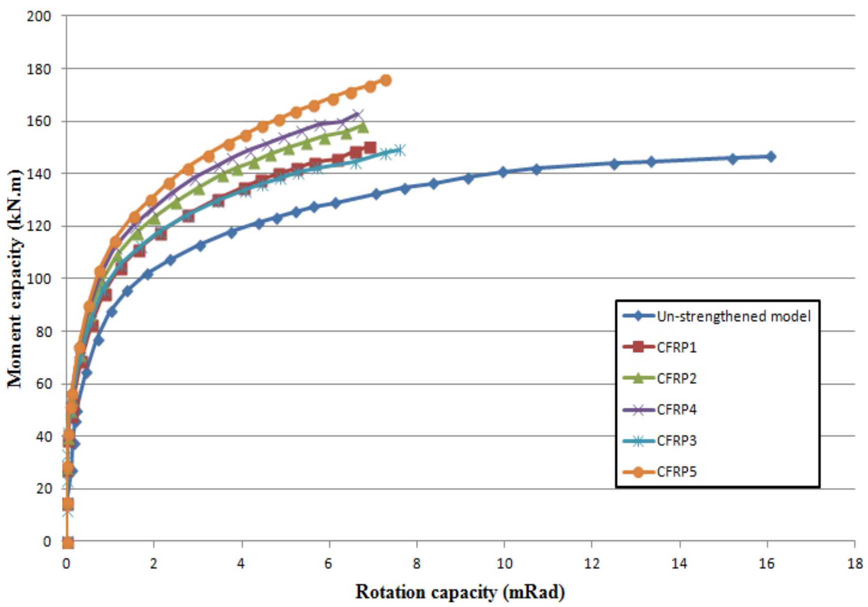

Figure 4.9 Moment-rotation curves for un-strengthened and strengthened models

Figures 4.10 through 4.12 show the stress contours in the ultimate moment capacity for bolts, column, and CFRP laminate in specimen CFRP5, respectively.

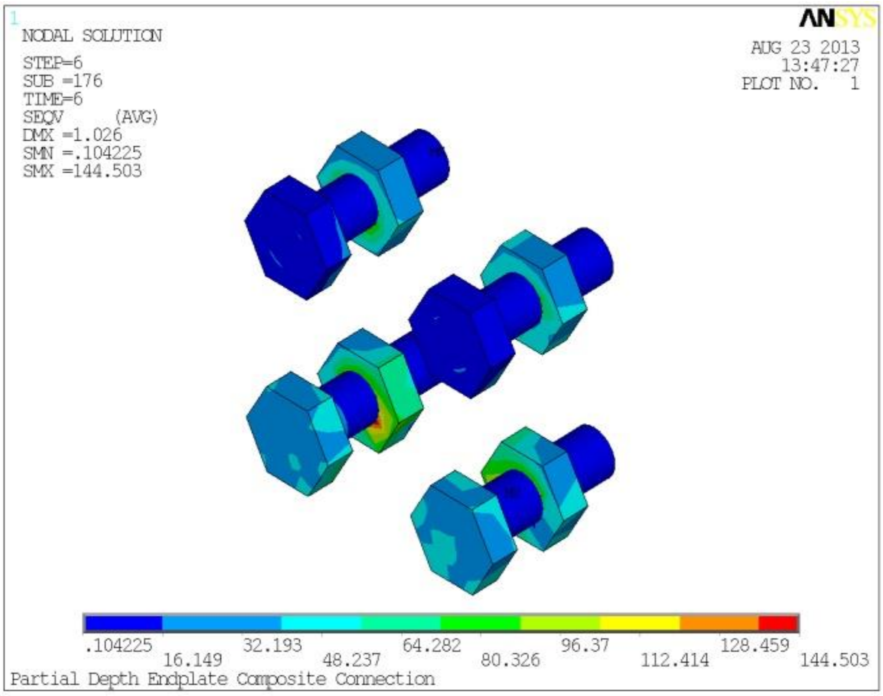

Figure 4.10 Bolts stress contour in ultimate moment capacity for CFRP5

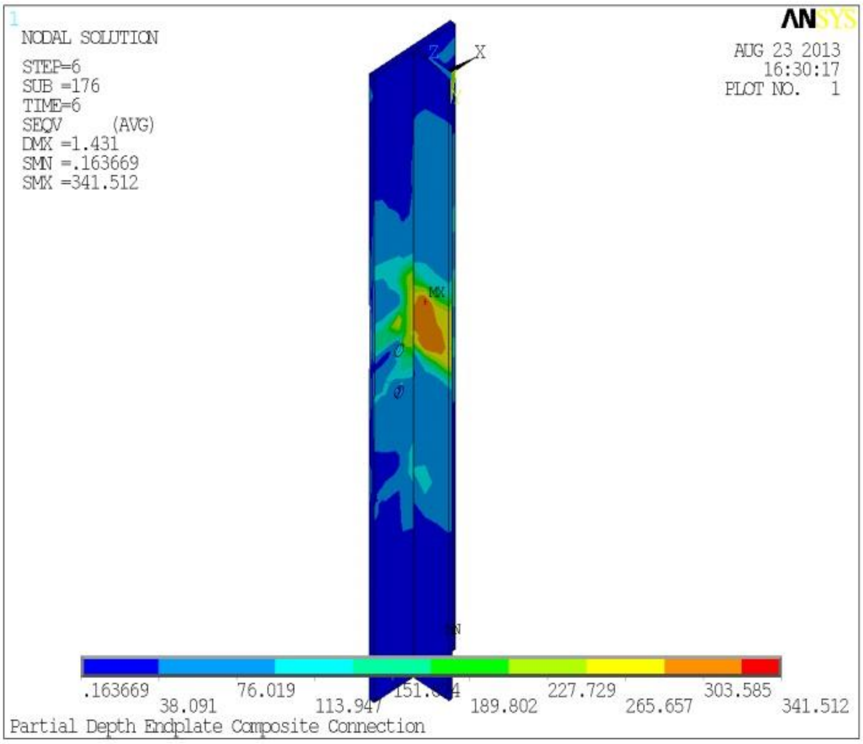

Figure 4.11 Column stress contour in ultimate moment capacity for CFRP5

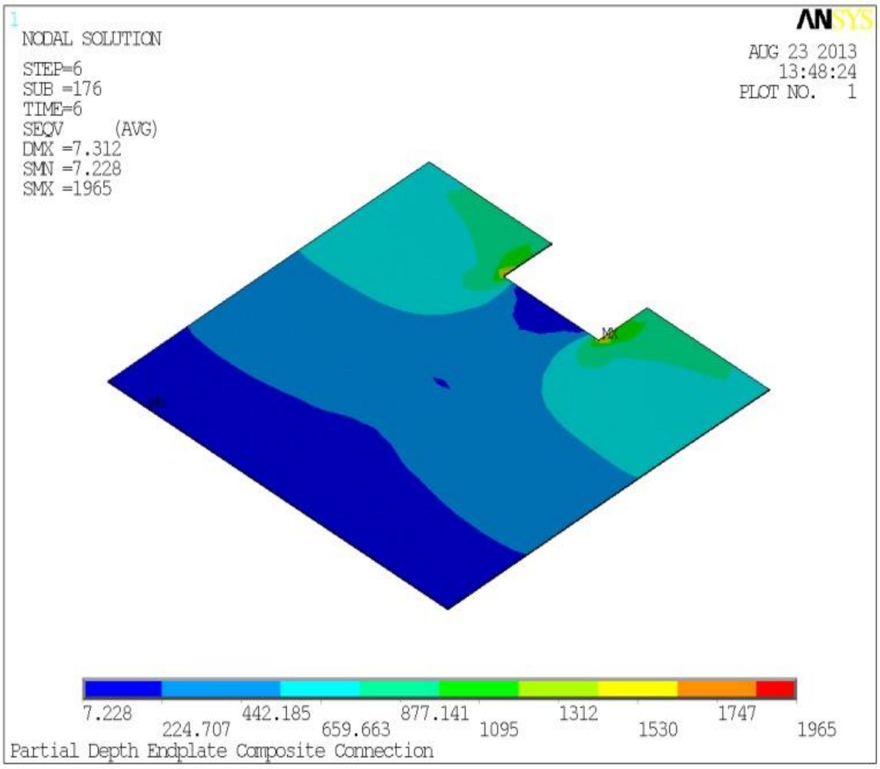

Figure 4.12 CFRP sheet stress contour in ultimate moment capacity for CFRP5

4.5 CFRP LAMINATE THICKNESS

In this study, to investigate the effect of the CFRP sheet thickness on the moment-rotation curve for composite connection, CFRP5 has been used with different sheet thickness. Table 4.4 shows the configurations of the models.

Table 4.4 Different CFRP laminates thickness

Test	CFRP sheet width (% slab width)	CFRP sheet length (% slab length)	CFRP sheet thickness (*mm*)
CFRP5	60	40	1.45
CFRP6	60	40	2
CFRP7	60	40	5

The moment resistance values for CFRP5, CFRP6, and CFRP7 are 175.919 *kN.m*, 176.158 *kN.m*, and 185.822 *kN.m*, respectively. The rotation capacities for these models are 7.264 *mRad*, 6.378 *mRad*, and 6.665 *mRad*, respectively. The results from the FEA are summarized in Table 4.5. From the results, it can be seen that by increasing the thickness of the CFRP sheets the moment capacity of the composite connection will be increased.

Table 4.5 Effect of CFRP sheet thickness

Specimen	Moment capacity (*kN.m*)	Rotation capacity (*mRad*)
CFRP5	175.919	7.264
CFRP6	176.158	6.378
CFRP7	185.822	6.665

The moment-rotation curves for these tests is plotted in Figure 4.13.

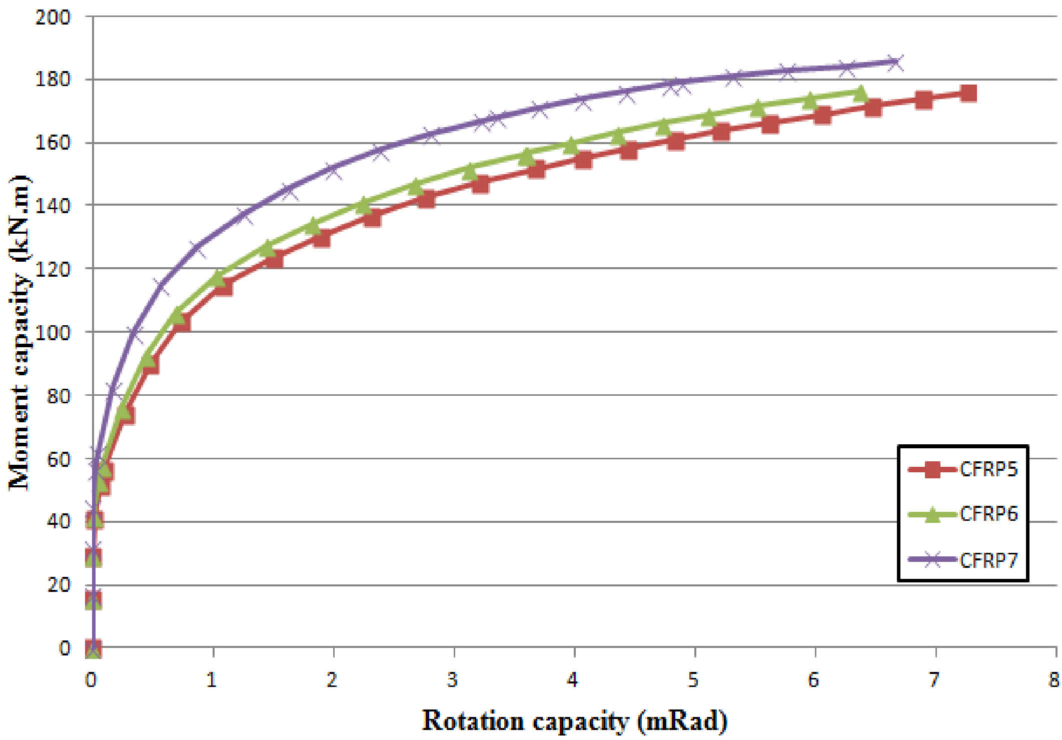

Figure 4.13 Effect of CFRP laminate thickness on the moment-rotation curve

4.6 REINFOREMENT BAR RATIO

To investigate the effect of the reinforcement bars on the composite connection, Test8 and Test9 with the same conditions but different reinforcement bar ratios from SCJ10 are considered. The reinforcement bar ratios for Test8 and Test9 are 0.2% and 0.4%, respectively. The results obtained from these finite element models are shown in Table 4.6 and Figure 4.14.

Table 4.6 Comparison of different reinforcement bar ratios

Test	Moment resistance (*kN.m*)	Rotation capacity (*mRad*)
Test8	113.931	9.11
Test9	126.604	8.612
SCJ10	146.469	16.045

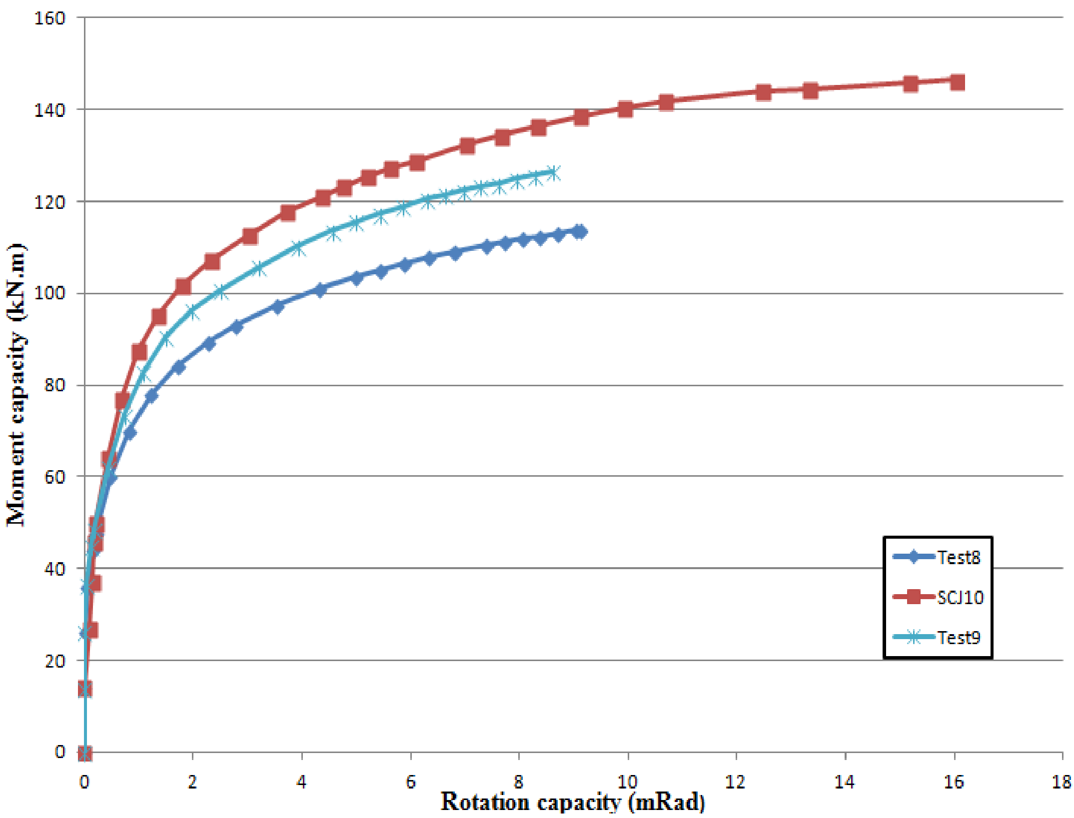

Figure 4.14 Moment-rotation curves for different reinforcement bar ratios

It can be seen that by decreasing the reinforcement bar ratio, the moment capacity will decrease. In addition, by decreasing the reinforcement bar ratio from 0.8% to 0.4% and 0.2%, the moment capacity decreases by 13.56% and 22.2%, respectively.

As stated, one of the main objectives of this study is to investigate the feasibility of decreasing the reinforcing bars in the presence of CFRP sheet in the tension face of the composite connection. The CFRP8 and CFRP9 are therefore considered. The specifications for these two models are shown in Table 4.7.

Table 4.7 Configurations for specimens CFRP8 and CFRP9

Test	CFRP sheet width (% slab width)	CFRP sheet length (% slab width)	CFRP sheet thickness (*mm*)	Reinforcement bar ratio (%)
CFRP8	60	40	1.45	0.2
CFRP9	60	40	1.45	0.4

Table 4.8 shows the results obtained from the finite element analysis for these two models.

Table 4.8 Moment-rotational response for CFRP8 and CFRP9

Test	Moment resistance (*kN.m*)	Rotation capacity (*mRad*)
CFRP8	142.774	3.233
CFRP9	149.97	3.688

Figure 4.15 compares the moment-rotation curves for the finite element models with different reinforcement bar ratios with and without incorporating CFRP laminates.

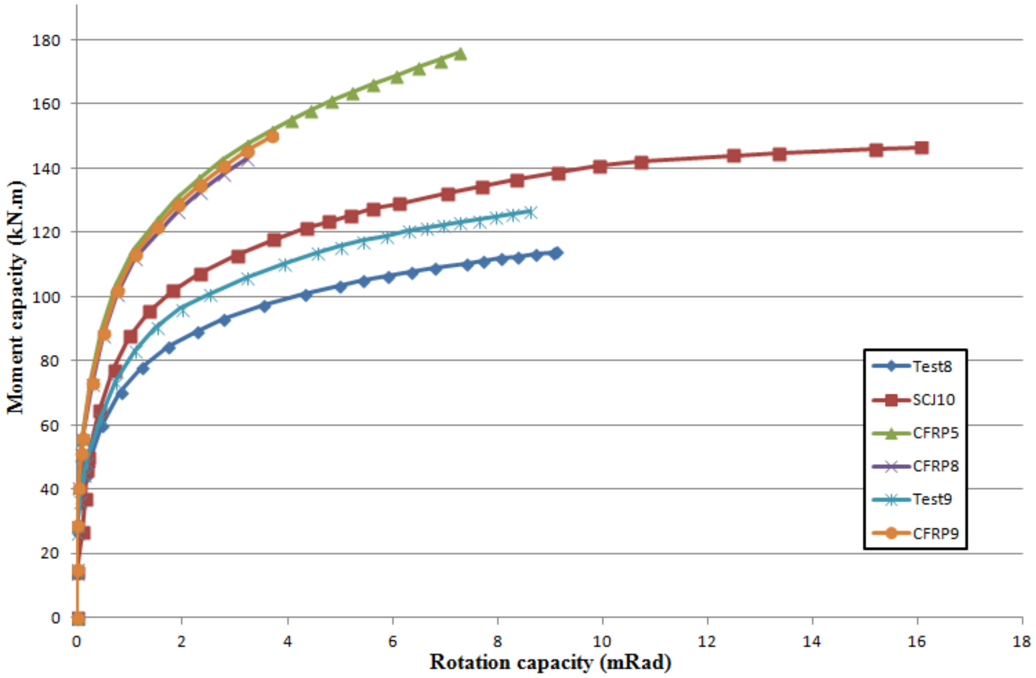

Figure 4.15 Moment - rotation curves with different reinforcement bar ratios, with and without CFRP laminates

From finite element results, it can be seen that the CFRP laminates can reduce the amount of reinforcement bars required for flexural strength. This will result in a simpler, less congested, and more economical joint details.

CHAPTER V

CONCLUSIONS AND RECOMMENDATIONS

5.1 CONCLUSIONS

A three-dimensional nonlinear finite element analysis was carried out using ANSYS software to obtain the moment-rotation curve. From this study it can be concluded that:

1. The moment-rotation curve produced by ANSYS software is shown to be similar to the one obtained in the experimental test. The moment resistance for the partial depth endplate composite connection obtained by ANSYS software is found to be very close to the corresponding laboratory test value with the percentage difference of about 3%.

2. The addition of FRP laminate reduced joint rotation by about 55% if the same load is applied to the joint with and without the overlay. Also, the increase in the thickness of the CFRP sheet could improve the performance of the composite beam-to-column connection by decreasing the joint rotation and increasing the moment capacity.

3. As mentioned earlier, the CFRP laminate can reduce the amount of reinforcing steel bars required for flexural strength of the composite connection.

5.2 RECOMMENDATIONS

Several recommendations are proposed for the future studies of endplate composite connections. The suggestions are as follows:

1. The laboratory tests should be done parallel with the modeling process to obtain a better understanding of the connection’s behavior and to make sure that all the data required for computer input is available.

2. The loading involved in the analysis of this research was monotonic. The fatigue analysis of the connection can be studied with cyclic loading.

3. The study on the bond stresses at the concrete-CFRP interface can be conducted.

REFERENCES

Abolmaadi, A., Malthys, J.H., Frooqi, M., & Choi, Y. 2005. Development of moment-rotation model Equations for flush end-plate connection, *Journal of Constructional Steel Research*, Elsevier

Ahmed, B., & Nethercot, D. A. 1995. Numerical Modelling of Composite Flush endplate Connections, Steel Structures, *Journal of Singapore Structural Steel Society*, Vol. 6, No. 1, pp. 87-102

Ahmed, B., & Nethercot, D.A. 1997. Prediction of initial stiffness and available rotation capacity of major axis composite flush endplate connections, *Journal of constructional steel research*, Vol. 41, No. 1 , pp. 31-60

Ahuja, V. 1982. Analysis of stiffened end-plate connections using the finite element method, *Master of Science Thesis*, School of Civil Engineering and Environmental Science, University of Oklahoma, Norman, Oklahoma

Al-Jabri K.S., Seibi A., & Karrech A. 2006. Modeling of unstiffened flush end-plate bolted connections in fire, *Journal of Constructional Steel research* Vol. 62, pp. 151- 159

Anania L., Badala A., & Failla G. 2005. Increasing the flexural performance of RC beams strengthened with CFRP materials, *Journal of construction and building materials* 19 (1): 55-61

Anderson, D., & Najaf, A. A. 1991. Semi-continuous composite frames in Eurocode4, *Connections in steel structures II*: Behavior, Strength, and Design

Anderson, D., & Najafi, A. A. 1994. Performance of Composite Connections: Major Axis End Plate Joints, *Journal of Construction Steel Research*, Vol. 31, No. 1, pp. 31-57

ANSYS, Release 12.1. 2009. *ANSYS Documentations, Manual Set and Theory Reference Manual.* ANSYS Inc.

Bahaari, M.R., & Sherbourne, A.N. 1994. Computer modelling of an extended end-plate bolted connection, *Computers and Structures* Vol. 52, pp. 879-893

Baharom, Sh., & Xiao, R.Y. 2011. Finite element analysis of composite beam with opening in metal-ribbed decking slab, *Australian Journal of basic and applied sciences* 5 (11): 1911-1923

Bennegadi, M.L., Sereir, Z., & Amziane, S. 2013. 3D nonlinear finite element model for the volume optimization of a RC beam externally reinforced with a HFRP plate, *Journal of construction and building materials* Vol. 38, pp. 1152-1160

Benussi, F., Puhali, R., & Zandonini, R. 1989. Semirigid joints in steel-concrete composite frames, *Construzioni Metalliche* n.5

Bijlaard, F. S. K., Nethercot, D. A., Stark, J. W. B., Tschemmernegg, F., & Zoetemeijer, P. 1989. Structural Properties of Semi-rigid Joints in Steel Frames, *IABSE Survey*, Periodical No. 2/89

Eldemerdash, M., Abu-Lebdeh, T., & Al Nasra, M. 2012. Finite element analysis of large capacity endplate steel connections. *Journal of computer science* 8 (4): 482-493

Garden, H.N., Quantrill, R.J., Hollaway, L.C., Thorne, A.M., & Parke, G.A.R. 1998. An experimental study of the anchorage length of carbon fiber composite plates used to strengthen reinforced concrete beams, *Journal of construction and building materials* Vol. 12,pp. 203-219

Gattesco, N. 1999. Analytical modeling of nonlinear behaviour of composite beams with deformable connection. *Journal of Constructional Steel Research* Vol. 52, pp. 195-218

Gergely, J., Pantelides, C.P., & Reaveley, L.D. 2000. Shear strengthening of RC-joint using CFRP composites, *Journal of Composites for Construction, ASCE*, 4 (2): 56-64

Gil, B., & Bayo, E. 2008. An alternative design for internal and external semi-rigid composite joints. part 1, *Journal of engineering structures* Vol. 30, pp. 218-231

Gil, B., & Bayo, E. 2008. An alternative design for internal and external semi-rigid composite joints. part 2, *Journal of engineering structures* Vol. 30, pp. 232-246

Heong, T.T. 2003. Design Appraisal of Steel-Concrete Composite Joints. *Doctoral Dissertation*, National University of Singapore

Ibrahim, A.M., & Mahmood, M.Sh. 2009. Finite element modeling of reinforced concrete beams strengthened with FRP laminates, *European journal of scientific research* ISSN 1450-216X Vol. 30 No. 4, pp. 526-54

Johnson, R. P., & Hope-Gill, M. 1972. Semi-rigid joints in composite frames, *IABSE Ninth Congress*, prelim Report, Amsterdam, pp. 133-144

Kheyroddin, A., Hoseini Vaez, S.R., & Naderpour, H. 2008. Numerical analysis of slab-column connections strengthened with carbon fiber reinforced polymers, *Journal of applied sciences* 8 (3): 420-431

Law, C. L. C. 1981. Planar no-sway frames with semi-rigid beam-to-column joints, *Ph. D. thesis*, Department of Engineering, University of Warwick, UK

Leon, R. T. 1990. Semi-Rigid Composite Construction, *Journal of Constructional Steel Research*, Vol. 15, pp. 99-120

Li, T. Q. 1994. The Analysis and Ductility Requirements of Semi-Rigid Composite Frames, *Ph. D. thesis*, University of Nottingham, UK

Li, T. Q., Nethercot, D. A. & Choo, B. S. 1996. Behaviour of flush endplate composite connections with unbalanced moment and variable shear/moment ratios: part 1: experimental behaviour, *Journal of Constructional Steel Research* Vol. 38, No. 2, pp. 125-164

Lu, X.Z., Jiang, J.J., Teng, J.G., & Ye, L.P. 2006. Finite element simulation of debonding in FRP-to-concrete bonded joints, *Journal of construction and building materials* Vol. 20, pp. 412-424

Maggi, Y.I., Goncalves, R.M., Leon, R.T., & Ribeiro, L.F.L. 2005. Parametric analysis of steel bolted end plate connections using finite element modeling, *Journal of constructional steel research* Vol. 61, pp. 689-708

Mosallam, A.S. 2000. Strength and ductility of reinforced concrete moment frame connections strengthened with quasi-isotropic laminates, *Composites: Part B: Engineering* Vol. 31, pp. 481-497

Mostofinejad, D., & Talaeitaba, S.B. 2006. Finite element modeling of RC connections strengthened with FRP laminates, *Iranian journal of science & technology*, Transaction B, Engineering, Vol. 30, No. B1

Najaf, A. A., & Anderson, D. 1992. Composite Connections with Structural Steel Endplate, *Final report to SCI,* Department of Engineering, University of Warwick, UK

Park, S.Y., Cho, K., Kim, S.T., Cho, J.R., & Kim, B.S. 2007. Behavioral characteristics of FRP-concrete composite deck in negative moment zones according to connection details, *Asia-pacific conference on FRP in structures*

Parvin, A., & Granata, P. 2000. Investigation on the effects of fiber composites at concrete joints, *Composites: Part B*, Vol. 31, pp. 499-509

Puhali, R., Smotlak, I. & Zandonini, R. 1990. Semi-Rigid Composite Action: Experimental Analysis and a Suitable Model, *Journal of Constructional Steel Research* Vol. 15, pp. 121-151

Queiroz, F.D., Vellasco, P.C.G.S., & Nethercot, D.A. 2007. Finite element modelling of composite beams with full and partial shear connection, *Journal of constructional steel research* Vol. 63, pp. 505-521

Richard Liew, J.Y., Teo, T.H., Shanmugam, N.E., & Yu, C.H. 2000. Testing of steel-concrete composite connections and appraisal of results, *Journal of constructional steel research* Vol. 56, pp. 117-150

Viest, I. M., Colaco, J. P., Furlong, R. W., Griffis, L. G., Leon, R. T., & Wyllie, L. A. 1997. Composite construction: *Design for buildings.* Wiley, *New York*

Wu, Ch., Zhao, X., Duan, W.H., & Al-Mahaidi, R. 2012. Bond characteristics between ultra high modulus CFRP laminates and steel, *Thin-walled structures* Vol. 51, pp. 147-157

Xiao, Y., Nethercot, D. A., & Choo, B. S. 1992. Moment resistance of composite connections in steel and concrete, Proceedings of the first world conference on constructional steel design, Acapulco, Mexico, November, pp. 331-343

Xiao, Y., Choo, B.S., & Nethercot, D.A. 1994. Composite connections in steel and concrete. part I, *Journal of constructional steel research* Vol. 31, pp. 3-30

Xiao, Y., Choo, B.S., & Nethercot, D.A. 1996. Composite connections in steel and concrete. part II, *Journal of constructional steel research* Vol. 37, No. 1 , pp. 63-90

APPENDIX

The moment-rotation response of specimen SCJ10 obtained from the finite element analysis software (ANSYS) is shown below.

Time	Moment capacity (kN.m)	Rotation capacity (mRad)
0	0	0
0.22222	14.2342	0
0.44444	26.8207	0.1
0.66667	37.1613	0.14
0.88889	45.9467	0.18
1	49.9034	0.21
1.3333	64.3208	0.42
1.6667	76.9233	0.684
2	87.5513	0.986
2.3183	95.3397	1.36
2.6517	101.752	1.81
2.985	106.914	2.312
3	107.133	2.335
3.35	112.864	3.022
3.7	117.785	3.731
4	121.253	4.357
4.2457	123.291	4.772
4.4957	125.316	5.195
4.7457	127.321	5.62
4.9943	128.811	6.069
5	128.854	6.1
5.1429	130.037	6.391
5.2857	131.061	6.716
5.4286	132.256	7.032
5.5714	133.364	7.354
5.7143	134.423	7.678
5.8571	135.243	8.023
5.996	136.275	8.335
6	136.311	8.344
6.1143	137.1	8.602
6.2286	137.832	8.866
6.3429	138.538	9.13
6.4571	139.23	9.395
6.5714	139.923	9.661
6.6857	140.603	9.926
6.8	141.201	10.199

6.9143	141.737	10.477
7	142.002	10.696
7.2823	143.02	11.416
7.4537	143.449	11.871
7.6823	143.972	12.48
7.7966	142.811	12.837
7.9109	144.228	13.105
8	144.612	13.328
8.2231	145.086	13.926
8.4517	145.409	14.557
8.6802	145.818	15.181
8.9088	146.215	15.805
9	146.469	16.045